1

Halogen Bonding: An Introduction

Daniel A. Decato, Eric A. John, and Orion B. Berryman

University of Montana, Department of Chemistry and Biochemistry, 32 Campus Drive, Missoula, MT 59812 USA

1.1 Introduction

The group 17 elements, known as halogens, are diatomic species in their elemental form with the chemical formula X_2 (where X = F, Cl, Br, I)[1]. In nature, they are seldom found in this manner due to their reactivity and thus are often presented as covalent or ionic species. However, the physical state of diatomic halogens provides initial insight into their capacity for noncovalent interactions. Moving down group 17, the elemental species exist in different phases from gas (F_2 and Cl_2) to liquid (Br_2) to solid (I_2). For simplicity, this observation is attributed to greater intermolecular dispersion forces afforded by the larger, more polarizable halogens and is quantifiable by physical properties such as boiling and melting point. This is the explanation that young chemists generally receive when being introduced to halogenated species and their physical properties. Later, in many organic curricula, these elements are presented as covalently bound components of molecules and are discussed within the context of molecular and bond dipoles, often in conjunction with concepts of electronegativity. Once again, the enhanced dispersion capacity of the halogens is often highlighted, explaining the higher boiling points of haloalkanes over hydrocarbons of comparable size and shape (e.g. ethane bp = −89 °C and bromomethane bp = 4 °C). Ultimately, the role of halogens in noncovalent interactions is neglected, giving way to their participation in classic reactions such as radical, substitution, and elimination pathways, which predictably leads to the misconception that halogens are simply electronegative leaving groups. This oversight is often reinforced in upper-level courses, where halogens are shown to be the reactive site in many cross-coupling reactions. Additionally, in classical inorganic chemistry, halides are depicted as weak field ligands and as prototypical examples in hard–soft acid–base theory. Even discussions of covalently bound halogens participating as hydrogen bond acceptors are atypical in university curricula.

1 The two other known halogens are astatine and tennessine. These two halogens are radioactive with short half-lives. Both are not often considered in the context of halogen bonding, although there has been some computational evaluation of astatine halogen bonding [1].

Halogen Bonding in Solution, First Edition. Edited by Stefan Huber.

In summary, halogens have traditionally been perceived as electronegative reactive species that participate in weak nondirectional noncovalent interactions (dispersion and as weak hydrogen bond acceptors). So how did scientists discover the ability of halogens to participate in a very directional and potent (comparable with hydrogen bond strength) noncovalent interaction, where the halogen is an electropositive species that is attracted to Lewis bases? To answer this, one should start with the definition of the halogen bond provided by the IUPAC in 2013 [2]. Then, early contributions from scientists who acknowledged an attractive interaction (more significant and directional than dispersion) can be acknowledged. Following the historical contributions, this introduction recounts the rediscovery of the halogen bond near the turn of the twenty-first century. Finally, the chapter concludes by highlighting impactful nonsolution-based examples that have helped construct the current understanding of the halogen bond, thereby providing context for the ensuing chapters on solution phase chemistry.

1.1.1 The Halogen Bond: Definition, Characteristics, Representations, and Parallels to the Hydrogen Bond

> *"A halogen bond occurs when there is evidence of a net attractive interaction between an electrophilic region associated with a halogen atom in a molecular entity and a nucleophilic region in another, or the same, molecular entity"*
> *IUPAC definition 2013* [2]

The depiction of a covalently bound halogen atom in traditional textbooks is that of an electron-rich sphere (Figure 1.1a). This simplified description is applicable in many cases and helps account for the behavior of covalently bound halogens as hydrogen bond acceptors [3] and their "side-on" interactions with metal cations [4]. However, the electron density around halogens is not uniform; the distribution of electron density is anisotropic, resulting in two regions of electron density [5, 6] (Figure 1.1b). The region directly involved in halogen bonding is the electropositive

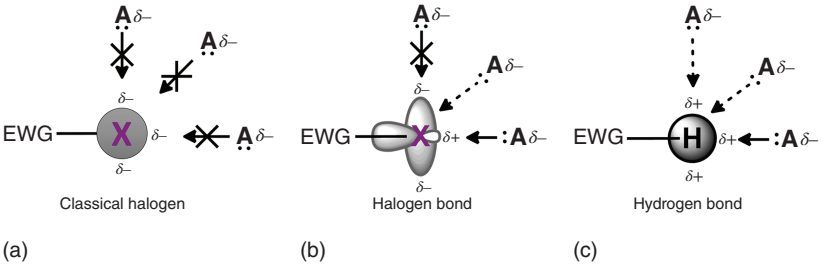

Figure 1.1 Schematic of interactions between a halogen atom and a Lewis base acceptor (**A**) from a classical view of halogens (a) and from a modern halogen bonding description (b). For comparison the depiction of a hydrogen bond is also included (c). A solid arrow indicates a "stronger" attractive interaction. The dotted arrow is a "less" attractive interaction. The solid arrow with an "X" through it indicates the interaction is repulsive.

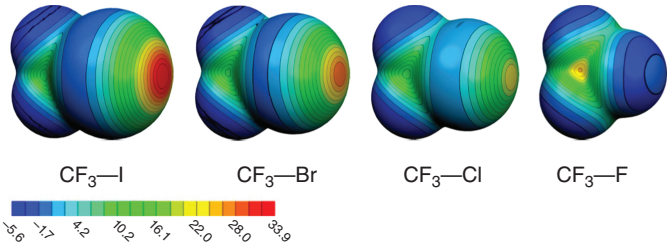

Figure 1.2 Molecular electrostatic potential maps drawn at the isodensity surface of 0.001 au for CF_3I, CF_3Br, CF_3Cl, and CF_4. All maps are drawn at the same scale, and values are in kcal/mol. Source: From Clark et al. [8]. © 2007 Springer Nature.

region at the tip of the halogen projected away from the covalent bond. This region is termed the sigma hole (σ-hole), *as it is a localized deficit of electron charge opposite a σ-bond* [7]. The second region is the electronegative belt, which forms orthogonal to the covalent bond involving the halogen atom. Thus, an electronic gradient on the surface of the halogen is formed, going from electropositive at the "tip" to electronegative around the equator. The electronic distribution is aptly demonstrated in Figure 1.2, which shows a series of molecular electrostatic potential (ESP) maps of trifluoromethyl halides [8]. Mapping halogenated species in this manner highlights the two distinct regions described above that engender the halogen bond with its characteristic directionality. For instance, if a Lewis base deviates from the σ-hole region, the interaction becomes less favorable and eventually becomes repulsive as the Lewis base approaches the electron-rich belt (Figure 1.1b). The σ-hole is most prominent in the CF_3I molecule and is depicted in this case as the red region of high ESP (Figure 1.2). The region can be quantified and compared with other systems by computing the maximum ESP ($V_{s,max}$) on the halogen.

Disclaimer: It is crucial to note that the σ-hole description does not account for all the nuances of the halogen bond. Therefore, other conceptual approaches and methodologies (e.g. polarizability, charge transfer) can and should be used to fully describe the halogen bond. These particulars are discussed in the computational section of this chapter. Nevertheless, the σ-hole is widely used, and ESP maps offer a low barrier to understand the general features and characteristics of the halogen bond.

1.1.2 Parallels to the Hydrogen Bond

The σ-hole concept elicits obvious parallels between the halogen bond and the hydrogen bond (Figure 1.1). As such, halogen bond studies, as well as concepts and nomenclature, were undoubtedly inspired by decades of hydrogen bond research. Similarities have prompted frequent comparison between the two, many of which are discussed in the following sections and ensuing chapters. A motivation of these comparative studies has been to discover the limits and unique features of this "new" noncovalent interaction. As such, studies in solution, solid state, and *in silico*

have already demonstrated promising features of the halogen bond compared with its hydrogen analogue.

1.1.3 Notation and Terminology

The vernacular of the halogen bond parallels the hydrogen bond. For example, the *hydrogen bond donor* references a molecule or group that contains a Lewis acidic hydrogen atom, while the *hydrogen bond acceptor* is the Lewis basic molecule or group in the interaction. In describing a halogen bond, the donor refers to the molecule with an electrophilic halogen atom (or simply the atom itself, for example, a *bromine donor*), and the halogen bond acceptor is the Lewis basic site. Therefore, the common notation for denoting a halogen bond is **R–X···Y**, where **R** is a covalently bound species, **X** is any halogen with an electrophilic region, **Y** is the halogen bond acceptor with an electron-rich region, and ··· indicates the attractive noncovalent interaction. Table 1.1 highlights common **R–X** species and several typical **Y** species.

1.1.4 Solid-state Halogen Bond Contacts

Halogen bond interactions in the solid state are typically quantified by their contact distance and angle with a Lewis base and described using the **R–X···Y** notation. Additionally, halogen bond contacts are often reported along with a percentage of their combined van der Waals (vdW) radii or more frequently a ratio. The ratio has been given various names such as the halogen bond interaction ratio, normalized interaction distance, normalized contact, or reduction ratio. The ratio is generally defined as $R_{XA} = \frac{d_{XA}}{(X_{vdW}+A_{vdW})}$ where d_{XA} is the measured distance (Å) from the halogen donor (X) to the acceptor (A), divided by the sum of the vdW radii (Å) of X and A ($X_{vdW} + A_{vdW}$). The ratio notation R_{XA} further informs the reader, as X is replaced with the atomic symbol of the halogen bond donor, while A denotes the atomic symbol of the halogen bond acceptor atom. For example, R_{BrO} indicates a halogen bond between a bromine donor and an oxygen acceptor. Reporting this ratio enables quick

Table 1.1 Common halogen bond donors and acceptors.

Common R—X species	• Dihalogen molecule (e.g. I_2, Br_2, ICl, ClF) • Haloalkane (e.g. CBr_4, CHI_3, $C_nF_{2n+1}I$) • Haloarene or heteroarene (e.g. iodobenzene, halopyridinium, and haloimidazolium cations) • 1-Haloalkyne (e.g. diiodoacetylene) • Halonium ion (e.g. diphenyliodonium or bromonium derivatives) • Haloimide (e.g. *N*-bromo- or *N*-iodosuccinimide)
Common Y species	Lone pair possessing atom (e.g. N atom of pyridine or an amine, O atom of a carbonyl group) π-System (e.g. double or triple bonds, arene moiety) Anion (e.g. halides, oxyanions)

Source: From Desiraju et al. [2]. © IUPAC.

comparison of distances between different halogen bonding sites; yet, it is important to specify the vdW values used as radii can differ based on the sources referenced [9]. Smaller ratio values typically indicate strong halogen bond interactions. When contacts involve anionic Lewis bases, some utilize ionic radii values [10], while others employ vdW radii. Presently, there seems to be no "industry standard," and simply reporting which values are used is the best practice.

1.1.5 Halogen Bond Features

Characteristics of the halogen bond have been established through experimental and theoretical means. From these studies several features of the halogen bond can be gleaned that should be considered in experimental and functional designs:

- The halogen bond is a highly directional interaction. The R–X· · ·Y angle tends to be close to 180°. This is due, in part, to the physical characteristics highlighted in Figures 1.1 and 1.2.
- The halogen bond is highly tunable, with energies up to 200 kJ/mol [11].
- Halogens are large atoms resulting in R—X bonds, which are longer than R–H counterparts (e.g. vdW radii of 1.46, 1.82, 1.86, 2.04, and 1.20 Å for F, Cl, Br, I, and H, respectively [9]).
- Halogen atoms are more hydrophobic than hydrogen atoms and the typical heteroatoms attached to them. Hydrophobicity of halogen atoms is a well-established phenomenon commonly utilized in drug development where the introduction of a halogen atom into a drug will often result in a drug that is more apt to cross lipid bilayers [12].
- Halogen atoms are more polarizable than hydrogens, providing the larger halogen bond donors with a suggested hard–soft acid–base complementarity with soft Lewis bases [13].

Despite the structural differences, both hydrogen and halogen bond donor strength can be tuned similarly by directly altering the donors (substituting heteroatoms and halogens, respectively) and by introducing stronger electron-withdrawing groups on the R group. Nevertheless, halogen bond tunability is achieved in various ways:

- By changing the halogen. A more polarizable halogen will result in a greater σ-hole (e.g. I > Br > Cl > F). This trend is illustrated in Figure 1.2.
- By changing the hybridization of the atom bound to the halogen. For example, with carbon, more s character increases the electron-withdrawing ability, resulting in a larger σ-hole on the attached halogen (e.g. $C(sp) > C(sp^2) > C(sp^3)$).
- By altering the atom, the halogen is bound to (e.g. N–I > C–I).
- By adjusting the electron-withdrawing ability of adjacent moieties. Increasing the electron-withdrawing ability of adjacent groups results in a greater σ-hole leading to, in most cases, a more potent interaction. The opposite is true as well – an electron-donating species will often diminish halogen bond strength.
- By noncovalent cooperativity. Noncovalent cooperativity is an emerging strategy to enhance the interaction strength of noncovalent forces. The introduction of

a hydrogen bond to the electronegative belt of the halogen further polarizes the halogen resulting in a more potent σ-hole resulting in a *hydrogen bond-enhanced halogen bond* [14–16].

1.1.6 Additional Nomenclature

Prior to the IUPAC definition of the halogen bond, a variety of terms were used to describe the attractive interactions with halogens, many of which have been pointed out by Bent [17]. One term used in early halogen bond studies referred to the interaction as a *donor–acceptor complex*, a consequence of the focus on charge-transfer studies. Thus, in many early papers, the halogen is referenced as an acceptor, signifying that the halogen was accepting electron density. This terminology has been mostly phased out when discussing halogen bonds. Other nomenclature found in the literature before the official IUPAC definition includes fluorine [18, 19], chlorine [20, 21], bromine [22], and iodine bonds [23, 24]. While this terminology does specify which donor is operating, the use of the more inclusive halogen bond term is the preferred method of representing the interaction. The field generally distinguishes between inorganic and organic halogen bond donors, as the interaction profile (e.g. electrostatic, charge transfer, dispersion) in these species is usually different. There are other specific notations that have been embraced within the community such as the term *charge-assisted halogen bond* [25–31]. The use of a formal charge, most often alkylation of Lewis basic sites (e.g. quaternization of amines), can result in a powerful electron-withdrawing group. If the history of the hydrogen bond is any indication, there will surely be new terminology that arises to describe other unique halogen bond interactions in the future. Already, the halogen bond field has examples of hydrogen bond-enhanced halogen bonds [14–16] and three-center-four-electron halogen bonds [32–34].

The above section has been constructed to provide the newcomer with a general understanding of the halogen bond. To enrich this knowledge, the following section chronicles key developments that provide context to the 2013 IUPAC definition.

1.2 Historical Perspective

To understand how the IUPAC definition of the halogen bond developed, one can look to the past. In fact, some have traced the observation of the halogen bond back to around the discovery of iodine. Consider what chemistry was probably like during the late Napoleonic era: mixing compounds, observing color changes, evolving gases, minimal safety concerns, etc. In fact, observing changes in color was how the first halogen bond complexes were detected (although not referred to as halogen bonds). The following is a brief commentary on a select number of historical studies considered to involve the halogen bond.

Early halogen bond observations occurred near the start of the nineteenth century in France, around the discovery and isolation of a new substance by Bernard Courtois in 1812. Samples of this material were given to a few chemists, including Sir

Humphry Davy and Joseph Louis Gay-Lussac. Shortly thereafter (December 1813), both Davy and Gay-Lussac identified (independently) and quarreled who was first to establish the new substance, iodine [35]. Less than a year later (July 1814), J. J. Colin, working for Gay-Lussac, reported the formation of a liquid with a metallic luster when mixing the newly identified material (I_2) with dry gaseous ammonia [36]. At the time the composition of the substance was unknown, but was eventually established by Frederick Guthrie in 1863 as *Iodide of Iodammonium* [37]. While the nature and atomic positioning of the two components remained unknown, Guthrie correctly predicted the formula of NH_3I_2. We now understand this material as a complex formed by a halogen bond between an iodine atom and the nitrogen atoms of the ammonia (I–I···NH_3). Similar 1 : 1 dimers between Br_2, Cl_2, and various amines were later reported by Remsen and Norris [38], while Rhoussopoulos provided initial evidence of iodoform participating in unique noncovalent interactions with quinoline [39].

The interest in I_2 continued into the early 1900s, resulting in numerous observations that are now understood to be rooted in the halogen bond phenomena. For example, Lachman in the early twentieth century noted various colors from solutions of diatomic iodine [40]. These colors range from brown or red brown solutions when combined with acetone, alcohols, ethers, amines, and benzene to more violet solutions with aliphatic hydrocarbons, carbon tetrachloride and chloroform. The diverse color palette of iodine solutions is now attributed to I_2···solvent complexes driven by the halogen bond. More importantly, studies of dihalogen complexes with various Lewis bases would have influences on two chemistry Nobel Prizes. The following few paragraphs will identify some of these impactful solution, solid, gas, and computational investigations leading to the rediscovery of the halogen bond in the late twentieth to early twenty-first century.

The works of Benesi and Hildenbrand in 1948 detailed that "…*new evidence has been found for the presence of addition compounds of iodine and the solvent molecule*" [41]. These studies evaluating aromatic hydrocarbons and their π-systems as acceptors (e.g. I_2···benzene) were influential in the development of conceptual models to explain halogen and Lewis base adducts. In fact, a couple years later in 1950, Mulliken evaluated carbonyl derivatives and ethers with diatomic iodine that helped developed electron donor–acceptor concepts used to understand these complexes [42]. A key component of the above studies was the use of UV–vis spectroscopy to closely monitor the changes, quantify behavior, and understand the nature of these early halogen bonded complexes. Ultimately, the widespread contributions of Mulliken led to him winning the 1966 Nobel Prize in Chemistry for "fundamental work concerning chemical bonds and the electronic structure of molecules by the molecular-orbital method" [43].

While many of these early studies observed spectroscopic changes, little was known about the atomic arrangements of these halogen bonding complexes. X-ray crystallographic studies began to reveal structural features of the halogen bond. Numerous cocrystal structures reported by Hassel in the 1950s were critical to elucidating structural features of the halogen bond. Early structures included Br_2···dioxane [44], Br_2···benzene [45], Cl_2···benzene [46], and Br_2···acetone [47]

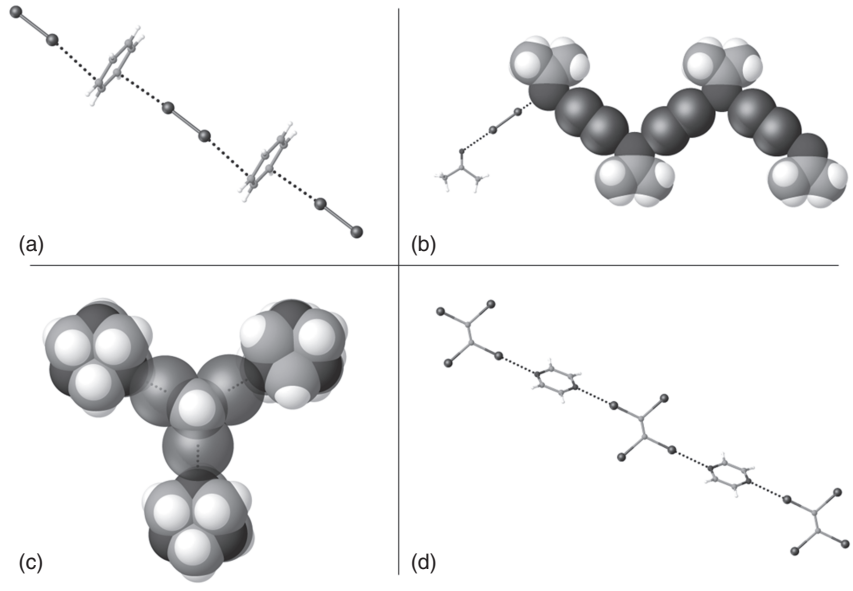

Figure 1.3 Early halogen bonding cocrystals from Hassel. Bromine/benzene adduct (a, BENZBR01), bromine/acetone adduct (b, ACETBR), hexamethylenetetramine/iodoform adduct (c, HEXAIF10), and tetraiodoethylene/pyrizine adduct (d, IETPYA10). CSD ref codes are provided after the location description. Dotted lines represent halogen bond contacts, and space-filling diagrams are drawn using default van der Waals radii in OLEX2.

adducts (Figure 1.3). Hassel noted the distinctive features of the halogen bond common to all solid-state studies: R–X· · ·Y angles of near 180° and contacts shorter than the sum of their respective vdW radii. Hassel's 1970 Nobel lecture provides perspective on early solid-state studies of halogen interactions and highlights themes still topical today such as hydrogen and halogen bond interplay [48]. In his lecture he also discusses a number of early halocarbon· · ·Lewis basic cocrystals such as 1 : 1 hexamethylenetetramine/iodoform adduct and 1 : 1 tetraiodoethylene/pyrizine adduct (Figure 1.3).

A definitive solid-state review written by Bent in 1968 compiles many early solid-state halogen bond studies [17] and highlights several characteristics that have been conclusively shown in modern studies. For example, Bent noted a hierarchy of interaction strengths highlighting contact distances of halogen bond complexes with diselenane (I_2 > diiodoacetylene > tetraiodoethylene). To expand the analysis, he compiled a hierarchy of donor and acceptor strengths from the compiled data (Figure 1.4). With the Cambridge Structural Database (CSD) recently surpassing one million structures, it is impressive to see that Bent was identifying and proposing trends from just 27 structures that were later verified to be correct (from much larger data sets).

In 1983 Dumas, Gomel, and Guerin presented a review primarily composed of various solution-based studies (e.g. UV–vis, nuclear magnetic resonance (NMR),

Table II

Relative donor and acceptor strengths determined from interatomic distances in addition compounds involving halogen atoms as electron-pair acceptors

Relative donor strengths

1. Toward bromine
   a. Dioxane > acetone
   b. Hexamethylenetetramine > acetonitrile
   c. Amines > ethers
2. Toward iodine
   a. Tetrahydroselenophene > diselena.ne
   b. Benzyl sulfide > dithiane
   c. Picoline ≈ trimethylamine
3. Toward iodine monochloride
   Pyridine ≈ trimethylamine
4. Toward diiodoacetylene
   Dioxane > cyclohexane-1,4-dione

Relative acceptor strengths

5. Toward dioxane
   a. Bromine > chlorine
   b. Chlorine ≫ oxalyl chloride
6. Toward dithiane
   Iodine ≫ diiodoacetylene > iodoform
7. Toward diselenane
   Iodine ≫ diiodoacetylene > tetraiodoethylene > iodoform
8. Toward amines
   a. Iodine ≈ iodine monochloride ≫ iodoform
   b. Bromine ≫ tetra.bromoethylene
   c. Iodine > bromine
   d. Bromine > iodoform > tetrabromoethylene
9. Toward molecular sulfur
   Iodoform > antimony triiodide

Figure 1.4 Table from the 1968 solid-state review by Bent. Source: From Bent [17]. © 1968 American Chemical Society.

Raman, IR) of intramolecular interactions of haloorganics with Lewis bases [49]. The message from this review was that the distinctive features of the halogen bond identified in the solid state persist in solution phase. One notable idea in the review was their consideration of halogen and hydrogen bond interplay in their solution studies: *The simultaneous presence of hydrogen atom(s) with acidic character and halogen atom(s) able to interact with a base leads to a new kind of "isomeric complex" in which the C–X···Y interaction competes with the C–H···Y interaction*. This observation is topical, and maintains to this day, a design consideration for modern solution-based halogen bonding chemists. To elaborate, many halogen bonding designs often incorporate strong electron-withdrawing groups to elicit stronger halogen bond interactions. However, in many instances, strong C—H hydrogen bond donors are also formed, highlighting a need to ensure molecule performance is largely dictated by halogen bonding and not C—H hydrogen bonding or other competing interactions. A modern study addressing this concern comes from the Huber lab [50].

Experimentally, the gas phase behavior of dihalogen bonding adducts with various Lewis bases was extensively studied by Legon using rotational microwave spectroscopy in the late 1980s and through the 1990s [51, 52]. They acknowledged the similarities between the hydrogen and halogen bond geometries in the gas phase but noted the distinct linearity of the latter. The study of these complexes in the gas phase revealed structural parallels to the solid state, reinforcing that halogen bond contacts were not a byproduct of lattice effects.

Contributing to the collection of halogen bonding data during this time were notable theoretical studies. The concept of the "σ-hole" discussed above was largely driven by the computational works of Politzer and Murray [5, 6]. Specifically, they demonstrated the anisotropic charge distribution of halogen atoms forming one covalent bond, the details of which are elaborated on in the computational section.

While not comprehensive, this section illustrates that the accumulation of data showing the attractive noncovalent behavior of halogens is consistent across the three primary phases of matter and *in silico*. These seminal studies and others provided the groundwork for the "rediscovery" of the halogen bond in the early 2000s.

1.2.1 Rediscovery

Dihalogens contributed extensively to the early identification of the halogen bond interaction. However, diatomic halogens (and interhalogens) limit the possible functional applications because they tend to be reactive and offer little in the way of tunability. This has led to the extensive study of haloorganics since the mid-1980s, as these species are readily adaptable to systematic study. For example, Weiss described interesting early instances of organic and cationic halogen donor complexes [53–55]. Additionally, a team from Politecnico di Milano in Italy, led by Pierangelo Metrangolo and Giuseppe Resnati, have studied many different haloorganics, including haloperfluorocarbons. Their contributions have aided in stimulating interest in halogen bonding. In particular, a review paper [56] and concept article [57] compile much of their early works and largely unify the field. The paper that many cite as the "rediscovery" of halogen bonding is titled "Halogen bonding: A Paradigm in Supramolecular Chemistry." Here, Metrangolo and Resnati describe several halogen bonding concepts that remain topical today such as hydrogen and halogen bonding selectivity, donor selectivity, acceptor selectivity, hard–soft acid–base favorability, the ability of the halogen bond to outcompete the hydrogen bond, and the ability of the halogen bond to perform admirably in aqueous media. This unification of halogen bond topics also details various methods for quantifying and identifying halogen bond interactions, including the use of heteronuclear NMR resonances (e.g. ^{14}N and ^{19}F). Lastly, they highlight several crystallographic studies providing the groundwork for the surge in subsequent solid-state halogen bonding studies. The design principles outlined by Metrangolo and Resnati highlight advantageous features of the halogen bond for the construction of predictable supramolecular architectures. For example, the effectiveness of dihalogen perfluorocarbons paired with various di-Lewis basic molecules to engender the formation of linear one-dimensional (1D) chains (Figure 1.5). Taken together, the studies

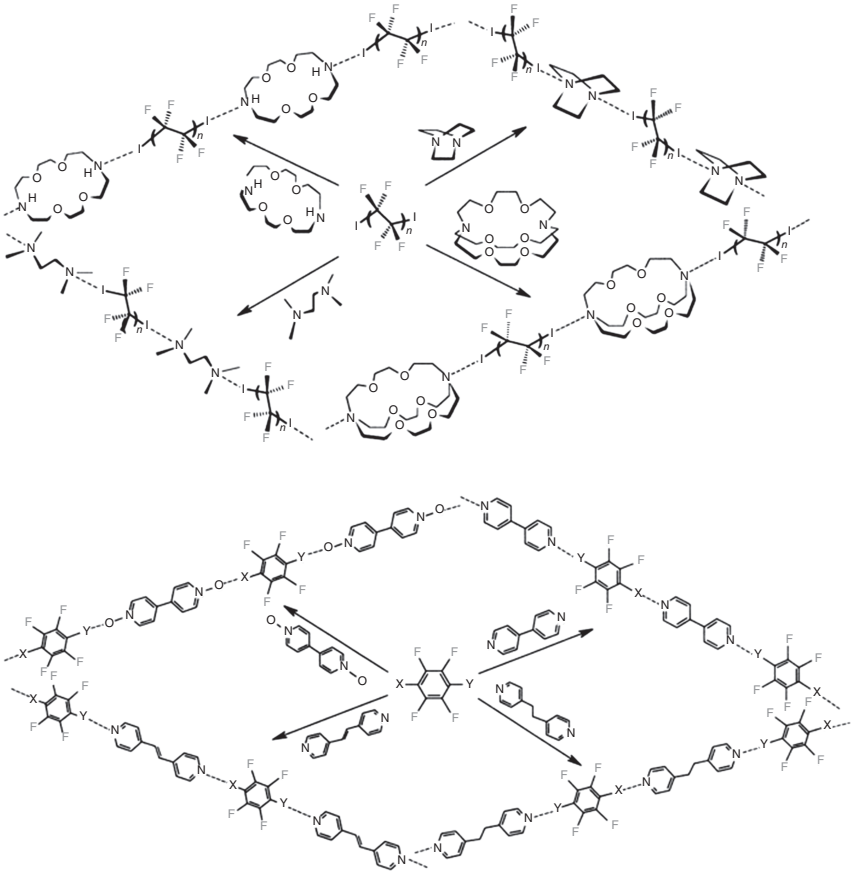

Figure 1.5 ChemDraw figure highlighting the use of alkyl- and aryl-dihaloperfluorocarbon halogen bond donors to form predictable 1D networks in the solid state. Source: From Metrangolo and Resnati [57]. © 2001 John Wiley & Sons.

from the groups of Metrangolo and Resnati have been instrumental in making the halogen bond topical to so many diverse research areas.

1.3 Crystallographic Studies

X-ray crystallography has been critical to establishing the field of halogen bonding and remains an integral part of modern analyses. Solid-state investigations often complement solution studies and provide perspective for the following chapters. For example, crystallography can reveal the atomic positioning of the atoms involved in a halogen bond. In fact, crystal structures will be presented in the ensuing chapters as they often reveal likely solution binding modes or binding stoichiometry. From a crystal engineering standpoint, the linearity of the halogen bond favors predictable structure directing contacts – a lauded feature that has been exploited in the construction of numerous 1D, 2D, and 3D halogen bond architectures [7]. In general,

solid-state studies have largely focused on fundamental investigations evaluating how this interaction "fits" into established crystal engineering concepts, the generation of new halogen bonding concepts, and application of the halogen bond in designed and functional crystalline materials. As such, this section is loosely organized from fundamental to functional studies and begins by highlighting a few CSD evaluations. The section provides a quick survey on halogen bonding in the solid state, and those desiring more extensive treatment of the topic are referred to the following reviews [7, 58–65].

1.3.1 CSD Evaluations

Possibly, the first CSD evaluation of what we now understand to be the halogen bond was in 1979 where the geometry of the C–I···O interaction was evaluated [66]. Murray-Rust and Motherwell noted an anisotropic distribution of contact distances as a function of C–I···O angle, where shorter contacts (and less variability) were observed for near linear (C–I···O $\angle \approx 180°$) contacts. The trend, although less pronounced, was also observed with Br and Cl species, which we now attribute to their weaker halogen bond donor ability. This initial study pulling from 20 000 structures was revisited again seven years later where the database had grown to 40 000 structures [4]. Here, Ramasubbu, Parthasarathy, and Murray-Rust evaluated halocarbons (C–X (X = Cl, Br, I)) and their contacts with metals, Lewis bases (nitrogen and oxygen species), and other halogens. The geometric characteristics of the "electrophile–nucleophile pairing(s)" showed that electrophilic metals favor a "side-on" approach to halogens, nucleophiles exhibited a "head-on" approach, and other halogens can participate as either the nucleophile (head-on) or the electrophile (side-on). These early CSD studies and others [67–69] reinforced the trends previously observed by Bent and Hassel, but observations from larger data sets provided more convincing conclusions.

Elaborating on halogen–halogen contacts, Parthasarathy and Desiraju established a classification scheme that is still used today [68]. The two contacts, type I and type II, are influenced by the anisotropic electron density and polarizability of halogens and have distinct geometrical conditions (Figure 1.6). The type II interaction is a true halogen bond – the electropositive portion of the halogen interacts with the electron-rich site of another. Type I contacts are considered geometry-based contacts that arise from close packing [62]. While not halogen bonds, the type I contacts

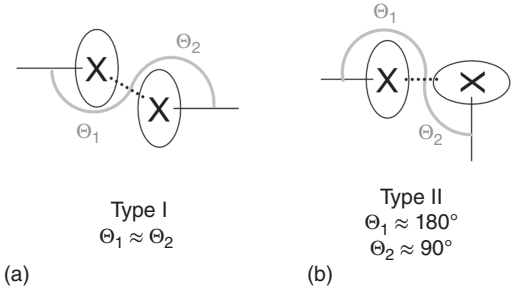

Figure 1.6 ChemDraw figure depicting the structural scheme for both type I (a) and type II (b) halogen···halogen contacts.

have been designed into solid-state structure and provide a convenient method of classification. The prefixes *cis*- and *trans*- have been recent additions to describe type I contacts, providing specificity of the arrangement of molecules in type I interactions [70]. A later report by Desiraju highlights a greater frequency of type II interactions following the donor atom species I > Br > Cl > F, further emphasizing that the type II contacts are true halogen bonds [62, 69].

1.3.2 Fundamental Studies and Halogen Bond–Hydrogen Bond Interplay

The CSD studies confirmed geometric trends from large amounts of data, further validating the characteristics of halogen bonds. However, several solid-state fundamental studies have demonstrated that the halogen bond is a tunable and predicable supramolecular tool. One example comes from Bruce and coworkers, where they systematically evaluated halogen bond distances between 4-(*N*,*N*-dimethylamino) pyridine (DMAP) and iodobenzenes with different degrees of fluorination [71]. Here it was shown that the I···N distance correlates with the degree of fluorination and with calculated pK_a values, signifying that the halogen bond is tunable for the construction of solids (Figure 1.7). The halogen bond angle (C—I···N) and distance largely correlate within these data; however there are some outliers that highlight the difficulties in constructing systematic solid-state investigations where many intermolecular interactions are at play.

Another systematic evaluation of halogen bond tunability comes from a collaborative study between Aakeröy, Metrangolo, and Resnatti [72]. These studies sought to rank common halogen bond donors. Initially, ESP maps of six ditopic halogen bond donor systems were computed to determine the $V_{S,max}$ at the σ-hole and establish a hierarchy of halogen bond strength (Figure 1.8). The values highlight how the σ-hole is influenced by the type of halogen, the hybridization of the carbon the halogen is bound to, and the degree of fluorination. More importantly, the $V_{S,max}$ rankings were correlated to the operating halogen bond donors in cocrystal structures. For example, when the halogen bond donor 1-(iodoethynyl)-4-iodobenzene is cocrystallized with 4-phenylpyridine, two halogen bond donor sites compete for a single Lewis basic site (only considering the pyridine nitrogen in this instance). The resulting structure shows that the better halogen bond donor (iodoethynyl) interacts with the pyridine nitrogen, while the weaker iodobenzene donor forms a type I halogen–halogen contact with an adjacent molecule (Figure 1.8b).

The above study suggests that the halogen bond can be used for hierarchical supramolecular synthesis. As such, the Aakeröy group began to consider adopting the hydrogen bond "best donor–best acceptor" concept to the halogen bond construction of crystalline solids [73]. pK_a values have been employed to help predict the best donor–best acceptor pairs for hydrogen bond cocrystals [74]; however, pK_a values are not readily adaptable to many halogen bond systems, leading to the use of ESP values. In one example of this concept transfer, ESP values for several multi-topic *N*-heterocyclic halogen bond acceptors were evaluated and cocrystallized with a diverse set of halogen bond donors [75]. The results

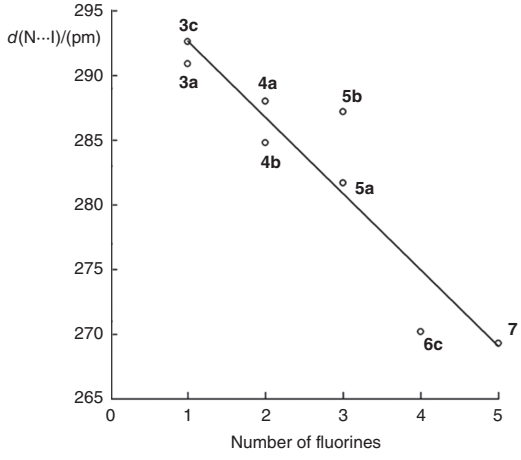

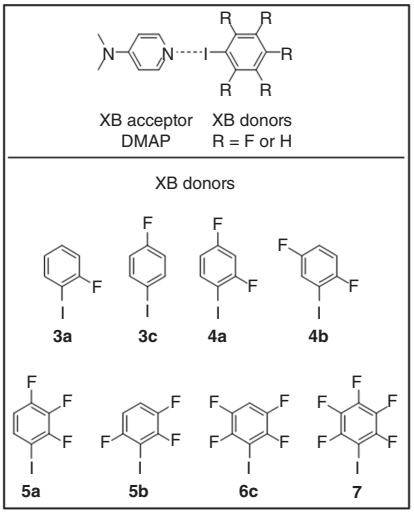

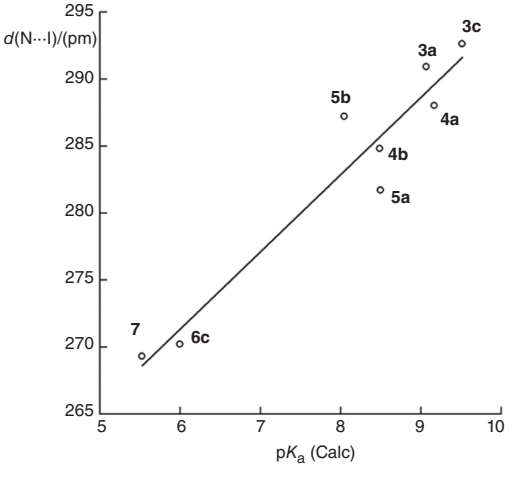

Figure 1.7 Halogen bond contacts between DMAP halogen bond acceptor nitrogen and iodine halogen bond donors of perfluoroarenes were evaluated. The various halogen bond donors with corresponding labels are shown in the middle bottom. Plot of N· · ·I distance versus degree of fluorination (left) and plot of N· · ·I distance versus calculated pK_a (right). Source: From Präsang et al. [71]. © 2009 American Chemical Society.

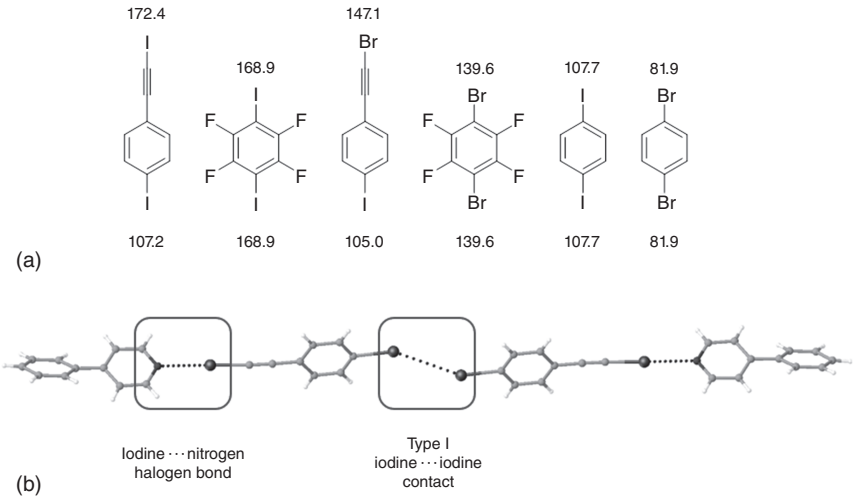

Figure 1.8 Six halogen bond donors were systematically evaluated computationally, statistically, and experimentally by Aakeröy et al. The reported values are the $V_{S,max}$ at the σ-hole region of the respective halogen in kilojoule per mole (kJ/mol), (a). Iodine atom interactions in the cocrystal structure of 1-(iodoethynyl)-4-iodobenzene and 4-phenylpyridine (b). CCDC ref code: BISBIQ. Source: From Aakeröy et al. [72]. © 2013 John Wiley & Sons.

highlighted that the site of larger negative ESP was the halogen bond acceptor in the crystal structure, paralleling the behavior of the hydrogen bond. By computing ΔE values (ESP difference) between the two Lewis basic acceptor sites, the authors were able to predict the site of halogen bond contacts. The study concluded that if ΔE was greater than 75 kJ/mol, then selectivity (best donor interacting with best acceptor) would occur. If ΔE was less than 35 kJ/mol, then no preference was observed, and often both acceptor sites would be occupied. Intermediate ΔE values were deemed to be unpredictable. ESP values were also adapted to systems that simultaneously use halogen and hydrogen bonds [76]. Here, a Q value was introduced (the Q value being the difference in ESP values of the halogen and hydrogen bond donor) to help predict which interactions would be present in the final structure. The donor molecules contain both halogen and hydrogen donors and were evaluated with a diverse set of acceptors in a series of cocrystals. It was reported that increasingly large Q values showed a tendency for only hydrogen bonding to be present as the main structure directing interaction. In contrast, lower Q values showed a greater chance of having both interactions operating. However, the authors note this is a "rule of thumb," and more work in this area needs to be conducted.

The simultaneous application of the halogen and hydrogen bond has also been evaluated so that they can coexist in the solid state. Here, Aakeröy has contributed tactics to avoid "synthon crossover" [77] by establishing supramolecular synthons that do not interfere with each other. Thus, higher-order cocrystallization may occur with greater frequency (e.g. ternary and quaternary cocrystals). In this light,

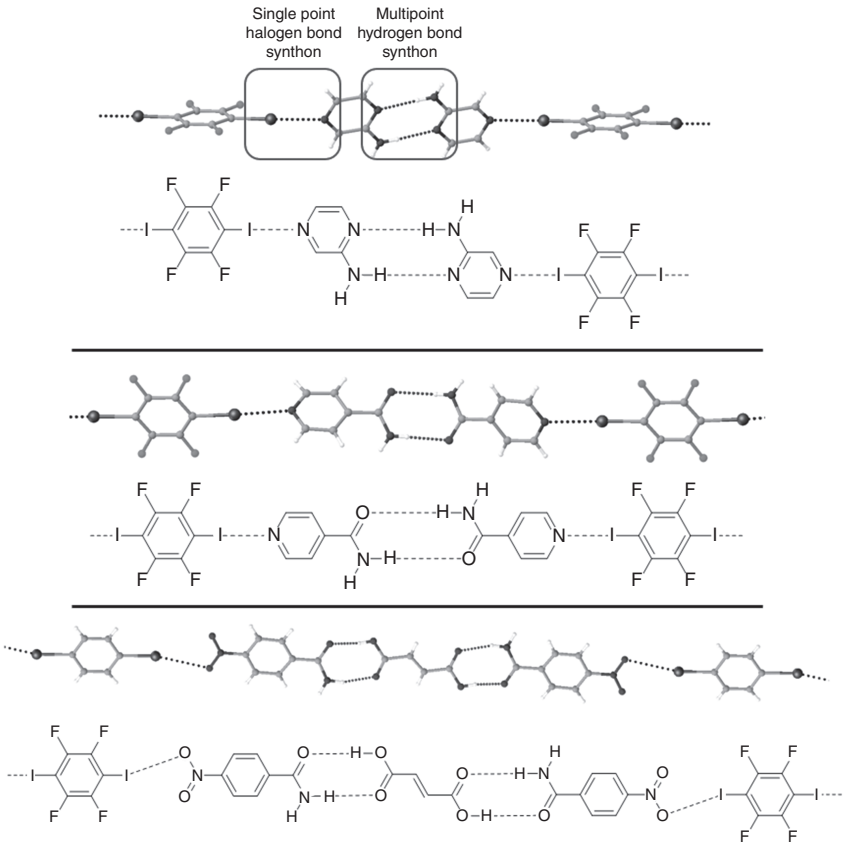

Figure 1.9 Examples of simultaneous halogen and hydrogen bonding in the construction of cocrystals. The top and middle figures highlighs the single-point halogen bond synthon and the multipoint hydrogen bond synthon. The bottom structure is an example of a ternary cocrystal assembly utilizing hydrogen and halogen bond synthons. Dotted lines represent halogen or hydrogen bonds. CCDC Ref codes: PAMLIA (top). (Aakeröy et al. [78].) YIPCIK (middle). PILLIH (bottom). (Tothadi and Desiraju [79].)

the halogen bond is a complementary interaction to employ alongside the hydrogen bond. This is because many hydrogen bond synthons are multipoint, whereas halogen bonds are often single point (Figure 1.9, top) [78]. This feature resulted in the successful construction of a number of cocrystals with simultaneous hydrogen and halogen bonds and is highlighted, in conjunction with other crystal engineering concepts, in ternary cocrystals such as those demonstrated by Tothadi and Desiraju in the (2 : 1 : 1) 4-nitrobenzamide/fumaric acid/1,4-diiodobenzene crystal structure (Figure 1.9, bottom) [79].

Simultaneous halogen and hydrogen bonding to carbonyl oxygens has also been of interest. A Protein Data Bank (PDB) study revealed geometrical orthogonality (X···O···H angle of $\approx 90°$) between the halogen and hydrogen bonds when simultaneously interacting with a carbonyl oxygen [80]. Computational analysis showed an energetic orthogonality, meaning that the strength of the hydrogen bond interaction

was not impacted by the halogen bond. This suggests that the halogen bond can be used as a recognition interaction without disrupting protein structures largely stabilized by hydrogen bonding. Small molecule analogues have also reproduced the geometric orthogonality [81], although Duncan et al. note some of the limitations of this feature [82]. Additionally, the observed geometric orthogonality between the hydrogen and halogen bond appears to be a somewhat general feature of carbonyls. A CSD evaluation highlighted that geometric orthogonality was persistent when two hydrogen bonds or two halogen bonds interacted with a single carbonyl, suggesting the observation is dictated by the carbonyl acceptor [83].

1.3.3 Metal Complexes and Charge-assisted Halogen Bonding Systems

So far, this chapter has described the use of neutral organic and neutral inorganic halogen bonding systems. The introduction of a formal positive charge results in a powerful electron-withdrawing group that can enhance halogen bond donor strength and can be achieved by protonation or alkylation of various heteroatoms (e.g. nitrogen, phosphorus). Similarly, coordinating a transition metal center has also been used to activate halocarbon halogen bond donors. The methods are highlighted in Figure 1.10 where halopyridine is used as an example. Methylation (or alkylation) of nitrogen heterocycles has been frequently employed, resulting in a diverse set of pyridinium, imidazolium, and triazolium donors that have been studied. An early example of activating a halogen donor by pyridine methylation comes from

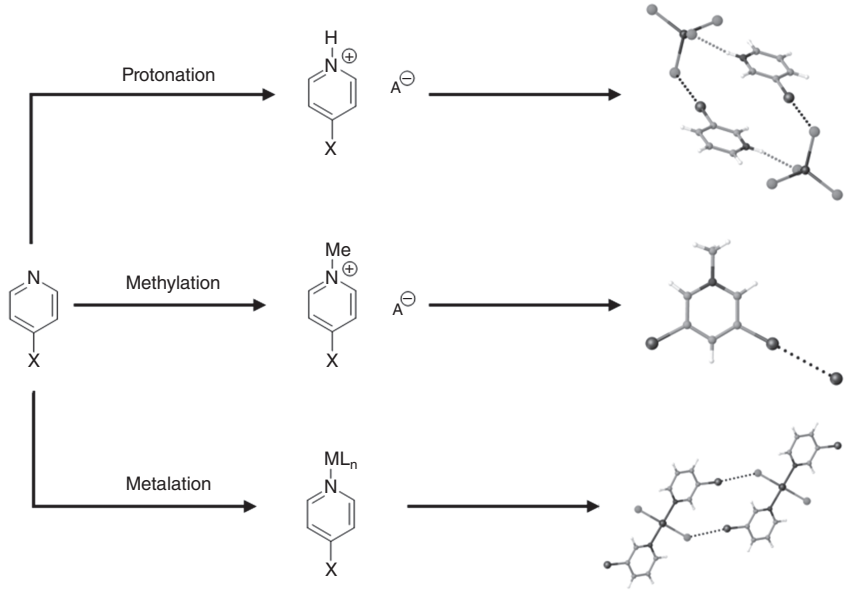

Figure 1.10 Methods to enhance the potency of a halogen bond donor. The ChemDraw figures provide a general description, while the ball-and-stick figures provide specific examples. Dotted lines indicate halogen or hydrogen bond contacts. CCDC ref codes: ALAJAY (top), BEYQIG (middle), RANSUV01 (bottom).

Resnati and coworkers who evaluated *N*-methyl-3,5-dibromopyridinium iodide (Figure 1.10, middle). The resulting crystal structure is highlighted by a helical structure formed between the cations and iodide [84]. The pyridinium, imidazolium, and triazolium systems noted earlier are frequently the subject of solution phase studies where solid-state evaluations offer complementary information. As such, the interested reader is referred to their discussions in later chapters.

The combination of halogen bonds and transition metal complexes has been evaluated by several groups [85–89]. Early work from Brammer involved the protonation of pyridine halides, resulting in simultaneous charge-assisted halogen and hydrogen bonding to perhalometallate ions (Figure 1.10, top) [90]. This would eventually lead to the construction of a classification system for crystal structures of halopyridinium···tetrahedral halometallate anion structures highlighting the tunability of the system from both the halogen bond donor and the halometallate acceptor [91]. The Brammer group also evaluated the activation of halogen bond donors through metal coordination, with an early study evaluating a family of compounds of the form *trans*-$[MCl_2(NC_5H_4X\text{-}3)_2]$ (M = Pt, Pd; X = I, Br, Cl, F) (Figure 1.10, bottom) [92]. Within this system, all structures exhibited M–Cl···X–C interactions, except complexes of fluoropyridine. Through their collective works, they have demonstrated that stronger halogen bonds are expected to occur with lighter metal halides. While no structures were reported, the Brammer lab has also produced halogen bonding studies of metal fluorides [93] and metal hydrides [94] in solution. The evaluation of nickel fluorides as halogen and hydrogen bond acceptors showed that the enthalpies of the interactions are similar (indole as the hydrogen bond donor, compared with iodopentafluorobenzene as the halogen bond donor). Studies of secondary sphere halogen bond interactions have been extended to other metal ligands such as the cyano ligand where the nitrogen lone pair of electrons acts as the halogen bond acceptor. A systematic study of halopyridinium–hexacyanometallate complexes highlighted that a decrease in X···N distances correlated with increasing metal d-electron count (Cr > Fe > Co) [95]. This was rationalized by greater π-back bonding to the cyano ligand. Halogen bonding to the secondary sphere of metal complexes has also been reported with the oxo-oxygens of the uranyl dication [96, 97].

The influence of halogen bonding on magnetic and conductive solids with redox properties has also been recently investigated. Halogen bonding tetrathiafulvalene (TTF) derivatives (molecular conductors) permit the variation of charge while maintaining the isostructural nature of halogen bonding units and have been the subject of several investigations by Fourmigué and coworkers [98, 99]. One example highlights a series of three isostructural complexes that vary the degree of charge transfer (neutral to ionic) between the TTF and tetracyanoquinodimethane derivatives, thereby directly showing the influence of charge on halogen bond strength [25]. The halogen bond has also played a role in the construction of nitroxide materials [100–102] and has been explored alongside ferromagnetic coordination polymers [103].

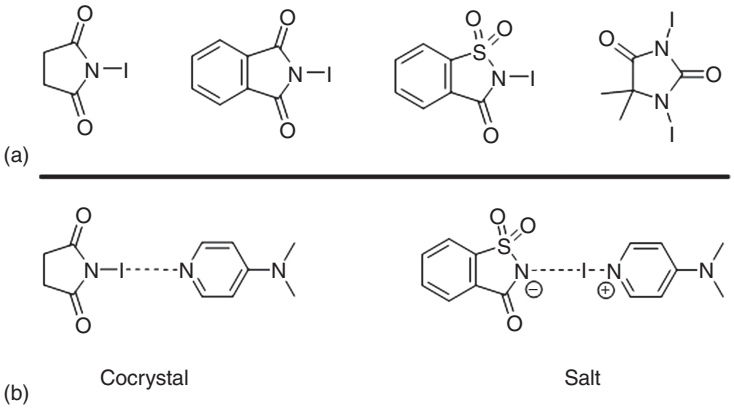

Figure 1.11 Representative examples of *N*-iodoimide halogen bond donors (a). Scheme of halogen bond cocrystal/salt concept transfer (b). ((b) Modified from Makhotkina et al. [105].)

1.3.4 Alternative Motifs and Solid-state Reactivity

The use of alternative or less common designs in halogen bonding has been reviewed [104]. Some of the less common donors include *N*-iodoimides (Figure 1.11a), which have been shown to be powerful halogen donors for a diverse range of acceptors [106–109]. In one example, Fourmigué and coworkers demonstrate that altering the donor and acceptor of these *N*-iodoimides can be used to demonstrate the cocrystal to salt continuum, a topic generally reserved for proton transfer between a hydrogen bond donor and acceptor. In the context of halogen bonding, it is iodine transfer that results in a salt (Figure 1.11b) [105] and has also been the subject of a charge density analysis study [109]. Another alternative halogen bond is the three-center-four-electron halogen bond of the type $[N—I—N]^+$. These unique motifs are often compared with the low barrier hydrogen bonds of the type $[N—H—N]^+$ and are the subject of an ensuing chapter.

Halogen bonds have also been used to mediate crystalline state reactivity. The first example of a photomediated [2 + 2] olefin cycloaddition was presented by Metrangolo and coworkers [110]. Here, a tetratopic halogen bond donor arranged *trans*-1,2-bis(4-pyridyl)ethene for cycloaddition using C—I···N halogen bonds (Figure 1.12, top). Similar tactics by Sinnwell and MacGillivray highlighted the use of a ditopic halogen bond acceptor to arrange the olefin-containing halogen bond donors, diiodooctafluorostilbene (Figure 1.12, bottom) [112]. Once again, C—I···N halogen bonds were employed to properly arrange the reactants. Only recently has a halogen bond cocrystal mediated a single-crystal-to-single-crystal transformation of an olefin cycloaddition [111]. The halogen bond has also been used to arrange polyacetylenes for polymerization. For example, the cocrystallization of 1,4-diiodo-1,3-butadiyne with either dipyridine or dinitrile oxalamide derivatives produced 2D networks driven by both hydrogen bond and halogen bonds [113] (Figure 1.13). The pyridine derivative only polymerized when subjugated to higher pressures, whereas the nitrile derivative polymerizes spontaneously at room

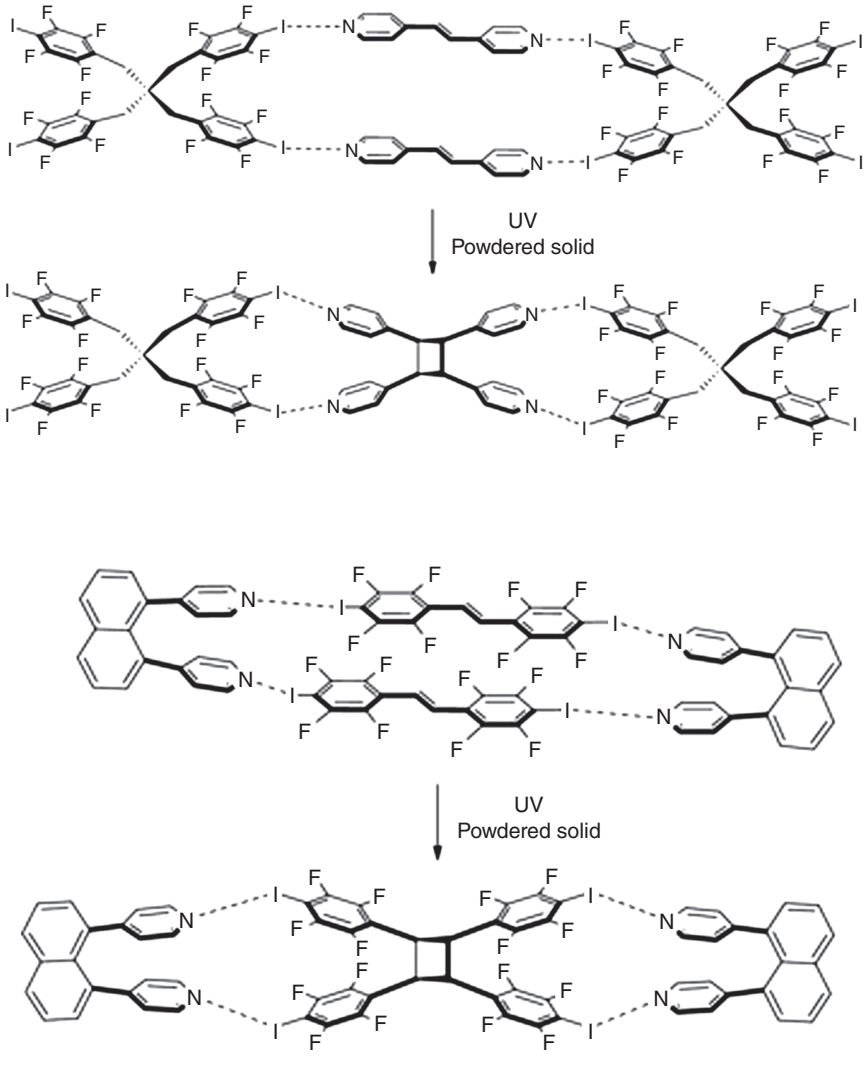

Figure 1.12 Examples of halogen bond mediated [2 + 2] photodimerization of olefins in the solid state. Source: From Sinnwell et al. [111]. Licensed under CC BY 2.0.

temperature (Figure 1.13). Solid-state reactivity can also occur by mechanochemistry or solvent-assisted grinding. For example, halogen bond-mediated cocrystals were produced with mechanochemistry using 1,4-diiodotetrafluorobenzene and 1,4-dibromotetrafluorobenzene halogen bond donors and analyzed through powder diffraction and single-crystal analysis [114].

1.3.5 Crystallographic Studies Conclusion

Solid-state evaluations of the halogen bond are vast, with numerous reviews written on the topic [7, 58–65]. This section provided a topical survey highlighting some

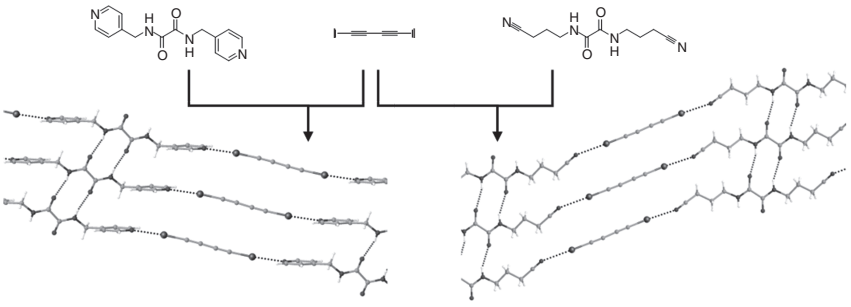

Figure 1.13 Cocrystallization components and pre-polymerization structures of 1,4-diiodo-1,3-butadiyne with oxalamide derivatives. CCDC ref codes: WANNUV01 (left), CEKFUU (right).

of the diversity within the field. However, one significant topic that was purposely omitted was halogen bonding to anions [115, 116] as many of the later chapters include aspects of halogen bonding to anions in solution (e.g. quantification, receptors, transport, catalysis). Other solid-state halogen bonding topics that have been omitted for brevity include solid-state NMR [117, 118], porous crystalline materials [119–121], crystalline rotors [122, 123], polyhalides [124–126], cosublimation [127], energetic cocrystals [127], and intramolecular halogen bonding [128]. Looking forward, crystallography will continue to be an important research tool that complements studies of halogen bonding in solution.

1.4 Computational Studies

1.4.1 Introduction

Computational chemistry has proven valuable to understanding the fundamental nature of the halogen bond and frequently complements observed experimental data. Computational studies have shown that different components (e.g. charge transfer, electrostatics, dispersion) contribute to the interaction and that the relative makeup depends on the nature of the halogen bond donor (e.g. inorganic, organic, neutral, charged assisted) and acceptor (e.g. neutral, charged, soft or hard Lewis base). In this section, the forces contributing to the halogen bond interaction and an overview of *in silico* methods used to study the halogen bond will be surveyed. For an in-depth look, reviews on computational halogen bonding theory in small molecule [8, 129, 130] and biological [131] systems have been published. Additionally, techniques to study the halogen bond (and other σ-hole interactions) *in silico* have been reviewed by Kozuch and Bickelhaupt [132] and Hobza [133].

1.4.2 Electrostatics of the Halogen Bond and the σ-Hole

One description of the halogen bond is rooted in the electron distribution of an isolated molecule within a ground state. As a polarizable halogen forms a covalent

bond with an electron-withdrawing group, a rearrangement of electrons results in electron-rich and electron-poor regions within the newly formed species. Consequently, the halogen adopts a spheroid shape, with the radius of the halogen extending from the covalent bond to the outer surface being smaller than the radius measured normal to the covalent bond (Figure 1.1b). The term "polar flattening" is sometimes used to describe the oblate shape of the electron cloud resulting from the depletion of electronic charge at the end of the halogen [134] and has been demonstrated in a CSD study [135] as well as by experimental charge density analysis [136, 137]. Polar flattening is not limited to halogens, but instead applies to all atoms covalently bound to another atom. Computationally mapping this distortion of electronic density has become a routine task and is achieved by measuring the ESP surface of a molecule. To better understand what ESP maps are depicting, it is necessary to outline their construction:

Equation 1.1 Electrostatic potential.

$$V(r) = \sum_{A} \frac{Z_{\mathrm{A}}}{\mid R_{\mathrm{A}} - r \mid} - \int \frac{\rho(r')\mathrm{d}r'}{\mid r' - r \mid} \tag{1.1}$$

ESP is an application of Coulomb's law and is a physical property that can be determined experimentally by diffraction techniques or computationally [138]. Given an electron density function $\rho(r')$, $V(r)$ is the ESP at any measured point r (Eq. (1.1)). Z_{A} is the charge on the nucleus that is located at R_{A}. $|R_{\mathrm{A}} - r|$ is the distance of the positive charge from r, and likewise $|r' - r|$ is the distance of the electronic charge from r, where r' is the integration variable over all space. A positive $V(r)$ indicates that effects by the nucleus are dominant or that the nucleus is not entirely shielded by the electron cloud. A negative $V(r)$ indicates that the electron density, in the form of electron pairs, π-bonds, etc., is dominant. ESP is frequently computed and viewed as a map covering the surface of a molecule. This surface is arbitrarily selected; however the most common surface to map is an outer contour of electron density, as it accurately encompasses lone pairs, strained bonds, and π-electrons (Figures 1.2 and 1.14). Typically, the $\rho(r') = 0.001$ au (electrons/bohr^3) contour is used, but other similar contours at 0.0015 or 0.002 au will also achieve the same ends [138]. The ESP values along this surface are then set to a color gradient directly on the molecule in question, and the extremes are typically represented as blue and red (Figures 1.14 and 1.2). While $\rho(r')$ and $V(r)$ are in Eq. (1.1), there is a distinct difference between the values. $\rho(r')$ is dependent on only electrons, while $V(r)$ incorporates contributions from all nuclei and electrons. As such, Politzer and Murray caution: *It cannot be assumed that high (low) electronic densities correspond to negative (positive) electrostatic potentials. The potential in a given region is the net result of negative contributions from the electrons and positive ones from the nuclei of the entire molecule, their effects of course being greater as they are closer to the region in question* [140]. In other words, ESP maps do not necessarily correlate with overall electron density.

Disclaimer aside, ESP maps are still highly informative. They have helped justify the amphoteric behavior of halogens observed in the solid state, where electrophiles approach the halogen "side-on" orthogonal to the C—X bond and nucleophiles

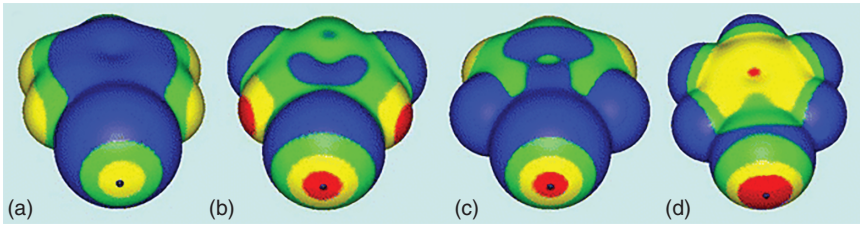

Figure 1.14 Computed ESP maps on 0.001 au molecular surfaces of (a) iodobenzene, (b) *meta*-difluoroiodobenzene, (c) *ortho*-difluoroiodobenzene, and (d) pentafluoroiodobenzene. Color ranges, in kcal/mol, are red, greater than 20; yellow, between 20 and 10; green, between 10 and 0; and blue, negative. Black hemispheres denote the positions of the iodine $V_{S,max}$. Source: From Riley et al. [139]. © 2011 Springer Nature.

Table 1.2 Table of iodine $V_{S,max}$ values and interaction energies (ΔE) of iodobenzene derivatives with acetone.

		Interaction angle	
		At (X···O=C) = 180°	At optimum X···O=C angle
System	$V_{S,max}$ (kcal/mol)	ΔE (kcal/mol)	ΔE (kcal/mol)
Iodobenzene	17.3	−2.44	−3.22
meta-Difluoroiodobenzene	26.1	−3.38	−4.13
ortho-Difluoroiodobenzene	25.5	−3.64	−4.71
para-Fluoroiodobenzene	35.9	−4.88	−5.97

Source: Adapted from Riley et al. [139]. Copyright 2011 John Wiley & Sons.

"head-on" in line with the C—X bond [4]. In particular, ESP studies by Politzer and Murray [5, 141] led to the establishment of the σ-hole concept, which has proven to be a widely valuable tool for conceptualizing the halogen bond and has contributed to the renaissance of other σ-hole-type interactions like chalcogen and pnictogen bonding [142]. Additionally, the ease of constructing ESP maps has led to their use in predicting relative halogen bond strength. For example, Politzer showed that the iodine $V_{S,max}$ values of iodobenzene derivatives largely positively correlate with their interaction energies with acetone [139] (Figure 1.14; Table 1.2). This relationship has been demonstrated a number of times theoretically [130, 143] and has led to the use of $V_{S,max}$ values as predictors of solid-state structures [72, 75, 144] and performance in solution [145]. Widespread application of $V_{S,max}$ and ESP maps has likely contributed to the halogen bond being mistakenly viewed as a purely electrostatic interaction; however other components are frequently important to fully describe the interaction [146]. For example, there are a number of cases where a more positive $V_{S,max}$ does not correlate with a stronger halogen bond [147].

1.4.3 Limitations on Electrostatic Potential

While ESP is an effective tool for predicting and conceptualizing interactions, there are limitations. Obviously, contacts that are not primarily electrostatic in nature cannot be accurately predicted, such as those reliant on polarization or charge transfer. Furthermore, ESP maps are only for isolated molecules and therefore do not account for other nuances when two molecules come together. For example, ESP maps do not calculate changes in electron distribution resulting from polarization due to incoming molecules. Therefore, to more accurately predict the strength of a halogen bond, more involved computational techniques that factor additional variables should be considered.

1.4.4 Atomic Orbital Theory and the σ-Hole

Formation of the σ-hole and the halogen bond interaction can also be described using atomic orbital theory. To paraphrase Clark, Murray, and Politzer, the electron-deficient σ-hole is caused by depleted occupancy in the outer lobe of a p-orbital of a covalent bond [8]. The halogen "X" has an $s^2p_x{}^2p_y{}^2p_z{}^1$ electronic configuration where the R—X bond is on the *z*-axis. In this electron configuration, two p-orbitals are filled, and one is half filled, thus highlighting the depleted electron density in the p_z orbital. This picture becomes more relevant with larger halogens and is more exaggerated when the halogen is covalently bound to an electron-withdrawing system. For example, this orbital character does not appear for fluorine. As fluorine is very electronegative, it shares more of the sigma bonding electrons, creating a higher degree of sp hybridization than larger halogens. Moving additional electron density into the p_z orbital affectively reduces the σ-hole. For example, in a C—F bond, 71.4% of electrons reside on F, whereas for less electronegative, larger halogens, like I, only ~50% of the electron density resides on the halogen [8]. Meanwhile, the σ-hole does not form for neutral, symmetric halogen containing molecules with equal electron distribution (e.g. carbon tetrahalides, hexahalobenzenes). This does not necessarily mean that symmetric or F-based systems do not form halogen bonds; rather other attractive components become the dominate force.

1.4.5 Charge Transfer

Charge transfer has long been associated with halogen bonding, and Mulliken's investigations of I_2 and organics containing O, S, or N heteroatoms are prime examples [42]. More recently, Palusiak utilized the Kohn–Sham molecular orbital (MO) theory to describe the interaction [148]. Halogen bonds and hydrogen bonds can have significant covalent character due to charge transfer from a guest to the antibonding σ* orbital (LUMO) of the R–X or R–H species [149] (Figure 1.15). The lower-energy σ* orbital and higher-energy σ orbital in this halogen bonding example allow for increased orbital mixing (σ orbital mixing shown for R–X donor in Figure 1.15b). These charge-transfer adducts often result in lengthening of

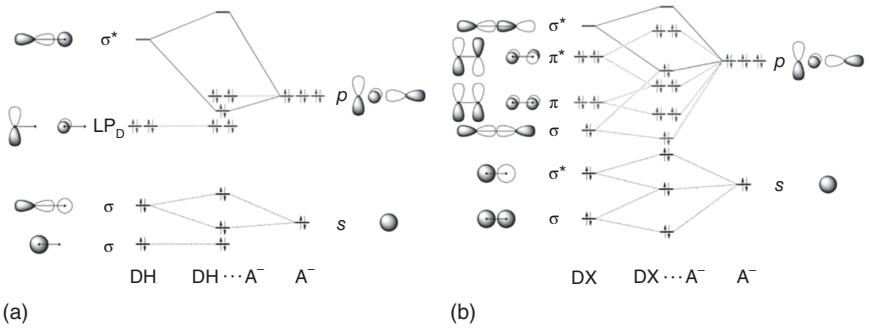

Figure 1.15 Simplified orbital-interaction diagrams for (a) hydrogen-bonded complexes DH···A⁻ and (b) halogen-bonded complexes DX···A⁻ as they emerge from quantitative Kohn–Sham MO analyses. Source: From Wolters and Bickelhaupt [149]. © 2012 John Wiley & Sons.

the R—X or R—H bond, which was highlighted in an early theoretical study of halogen bonding complexes between dihalogens (including interhalogens) and Lewis bases [150]. Here, elongation of the halogen–halogen bond is largest in the strongest complexes, up to 0.065 Å in the $FBr\cdots NH_3$ complexes. The study also demonstrated that the most polarizable halogens, and the interhalogens (FBr, FCl, etc.) with the biggest dipole, resulted in the largest interaction energies. Other studies have revealed that charge transfer can be a significant factor in organic halogen bond systems as well. One example evaluated complexes of bromocarbons (e.g. CBr_3F, CBr_3NO_2, CBr_3COCBr_3, CBr_3CONH_2, Br_3CCN) with anions (Br^-, N_3^-, NCO^-, and NCS^-) [151, 152]. In these reports, increasing charge transfer was linearly correlated with elongation of the C—Br bond length. Therefore, as the interaction strength with the Lewis base increases, the C—Br bond lengthens, suggesting that the donation of electrons to the antibonding σ* from the p-orbital of the Lewis base results in a weakening of the C—Br bond. These conclusions are further supported by MO theory where charge-transfer effects are the leading component for organohalogen halogen bond formation in $H_3C—X\cdots O{=}CH_2$ and $F_3C—X\cdots O{=}CH_2$ (X = Cl, Br, I) models [148].

1.4.6 Dispersion and Polarization Component

London dispersion and polarization effects on the halogen bond can be important given the polarizability of larger halogens (e.g. I and Br) and the fact that interacting partners are frequently closer than the sum of the vdW radii. Dispersion interactions resulting from a temporary dipole and another dipole between the halogen and Lewis base provide a small but attractive force that contributes greatly in systems without large electropositive σ-holes [153].

Lump–hole theory [154] is an alternative electrostatic model that describes a depletion of negative charge at the end of the halogen and accounts for dispersion and polarization. For example, Hobza and coworkers showed that a CH_3Cl molecule can form a halogen bond with $O{=}CH_2$ despite that the Cl never forms

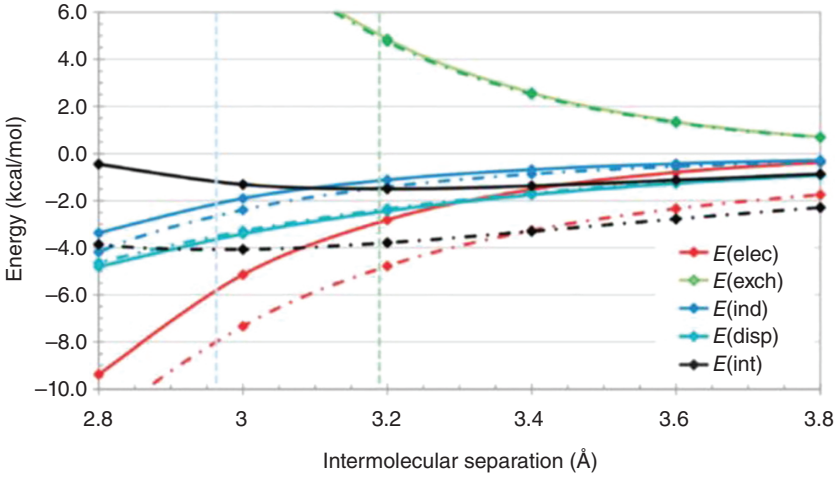

Figure 1.16 DFT–SAPT decomposition analysis of $H_3CBr\cdots NH_3$ (solid lines) and $F_3CBr\cdots NH_3$ complexes (dashed lines) (kcal/mol). Potential energy minima are shown as vertical dashed lines ($H_3CBr\cdots NH_3$ is green, and $F_3CBr\cdots NH_3$ is light blue). The components are reported as follows: electrostatics (*E*(elec)), induction or polarization (*E*(ind)), dispersion (*E*(disp)), and exchange (*E*(exch)), and total binding energies (*E*(int)). Source: From Riley and Hobza [153]. © 2013 Royal Society of Chemistry.

an electropositive σ-hole [155]. Obviously, σ-hole theory does not account for weak halogen bond formation in CH_3Cl as dispersion dominates the interaction in this case.

1.4.7 Decomposition

With decomposition analysis of intermolecular forces, contributions of electrostatics, induction or polarization, dispersion, and exchange repulsion are quantified. Decomposition of the halogen bond has allowed researchers to obtain a more complete view of the halogen bond. Symmetry-adapted perturbation theory (SAPT) [156] and the density functional theory version (DFT–SAPT) [157] are used to describe the bonding components of the halogen bond. Total decomposition of the $H_3CBr\cdots NH_3$ and $F_3CBr\cdots NH_3$ halogen bond adducts (Figure 1.16) reveals notable differences between the two [153]. Specifically, the CH_3 derivative was largely driven by inductive and dispersive forces, whereas the inclusion of CF_3 groups led to a significantly larger electrostatic contribution.

1.4.8 Biological Computation of Halogen Bonding

Utilizing the halogen bond in biological settings is still novel. Currently, researchers are evaluating the influence of halogen bonding in protein stability, substrate binding, and drug design. Although nature seldom employs the halogen bond [158], medicinal chemists have found that the hydrophobicity of the halogen and directionality of the halogen bond could improve drug delivery and specificity. Drug design

is time and cost intensive. To reduce this, medicinal chemists frequently turn to computational chemistry to identify target systems. However, specialized tools for modeling the halogen bond are still rare in the field.

Ho has been at the forefront of studying halogen bonding in biochemical systems. Using experiments, computations, and PDB searches, his group revealed that halogen bonds can stabilize ligand binding and molecular folding in proteins and nucleic acids [159]. An initial survey of the PDB found 113 different interactions when searching for short halogen-Lewis base interactions. To date, more than 790 structures featuring the halogen bond in the PDB have been found [160]. A review by Ho et al. has also summarized current computational designs for halogen bonding drug candidates [161]. Using the structure of a protein and its binding pocket, their methodology identifies possible halogen bond acceptors within the pocket and predicts optimal positions to place the halogen bond donor. This tactic allows medicinal chemists to predict which donor to incorporate and where to place it on a substrate. Hobza has used another approach by employing the semiempirical family of PM6 functions to make halogen bond computations accessible without using computationally expensive quantum mechanical (QM) calculations [162, 163]. Using this method, they demonstrated that reasonable modeling can be achieved using lower levels of theory on non-halogen bonding components.

Other methodologies for studying the halogen bond in biology are effective and highly utilized. For example, Boeckler developed an evaluation tool called XBScore, which rates halogen bond interactions in proteins using QM/molecular mechanics (MM) calculations [164]. QM/MM uses computationally cheap MM to model most of the protein and expensive QM to model the binding site and halogen bonding substrate [165]. In comparison, other techniques like optimized potentials for liquid simulations-all atoms (OPLS-AA) [166] or assisted model building with energy refinement (AMBER) [167] have used a positive extra point approach by adding a pseudoatom at the halogen atom surface to inexpensively simulate a σ-hole. Ho further developed these force field systems by deriving MM/MD equations specifically for the halogen bond [168]. The above computational techniques highlight how the ingenuity of the chemists has overcome limitations of computational power to provide reasonable predictions in a timely fashion.

1.4.9 Computational Conclusion

To date, researchers have generated a variety of computational and experimental tools to study the halogen bond, and they are constantly being improved. One can look at the aphorism by the statistician George Box, which states, “All models are wrong, but some are useful.” Computational models depend on the experimental systems they come from and make assumptions to limit the computational resources required. However, these limitations are being lifted to obtain useful information for drug design and fundamental interaction studies. Future halogen bonding computational models will be developed, which combine the better processing power of future hardware with a greater understanding of the principles that make up the halogen bond. Computational studies of the halogen bond and other noncovalent

interactions will be necessary for rational molecular design across many synthetic fields. Furthermore, these studies provide a strong foundation to understand the solution-based halogen bonding presented in later chapters of this book.

1.5 Materials

1.5.1 Introduction

Materials like liquid crystals (LCs), polymers, and gels frequently exhibit properties governed by noncovalent forces, most often the hydrogen bond. As expected, the distinct characteristics of the halogen bond, such as high directionality, strength, polarizability, and hydrophobicity, provide enticing prospects for the development of novel materials. In this section, select examples of halogen bonding materials are presented. For more information pertaining to halogen bond materials, recent reviews have been published [7, 169].

1.5.2 Liquid Crystals

The LC state is a mesophase, having properties of both crystalline solids and isotropic liquids, with extensive real-world applications. A variety of different noncovalent interactions are employed to achieve desired LC properties (e.g. low temperature formation, unique light modification, predictable phase transition, etc.), but hydrogen bonding is by far the most common [170]. The success of hydrogen bond-mediated LCs is largely attributed to its directionality, thereby inspiring evaluations using the more stringent halogen bond. In fact, LCs incorporating halogen bonds have exhibited unique properties dissimilar to hydrogen bonding derivatives. This section provides select examples of how the halogen bond has been applied to produce different classes of LCs. For further reference, a recent review of the topic has been published [171].

The first example of LCs assembled by halogen bonding was reported by the Bruce lab in 2004 [172]. Here, alkoxystilbazole derivatives were used as halogen bond acceptors and pentafluoroiodobenzene as the donor (Figure 1.17). X-ray crystallographic studies suggested the LC formation resulted from a C—I···N halogen bond. The dimeric complex formed LCs only when cooling, known as monotropic formation. However, alkoxystilbazoles with longer alkyl chains ($n > 6$) resulted in enantiotropic LCs (occurring at both heating and cooling cycles). Exchanging the iodine donor for a weaker bromopentafluorobenzene precluded LC formation. The LC formation temperature was lower for the halogen bond derivatives than hydrogen bonding analogues – a property that is generally beneficial for LCs

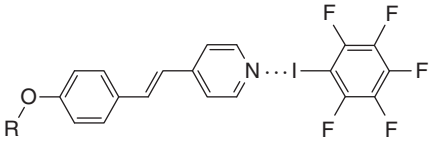

Figure 1.17 The first example of a halogen bonding LC developed by Bruce. Alkyl chains R related to LC behavior.

operating near room temperature (e.g. liquid crystal display [LCD] displays). Many other early halogen bond LCs incorporated iodoperfluorobenzene donors, as they form moderately strong halogen bonds and are readily available for purchase [173–176]. However, in 2013, Bruce used molecular iodine as a halogen bond donor to create LCs with stilbazole acceptors [177]. The high temperature stability (>200 °C) of the mesophase was attributed to the intermolecular iodine–iodine contacts. These initial examples demonstrate the ability of the halogen bond to facilitate LC formation with favorable properties.

The Bruce lab, along with Metrangolo and Resnati, also contributed to the first example of ionic LCs using halogen bonds [173]. Using tricomponent imidazolium cations and neutral perfluoroiodo halogen bond donors bound to iodide, they showed that the alkyl chains on the organocations did not drive liquid crystallinity and even smaller chain lengths ($n = 2$) formed a mesophase. Later studies made these systems light responsive [178].

Photoresponsive LCs, used in displays, nanotechnology, and photo-driven devices, provide on–off switchable liquid crystallinity. Toward this end, the halogen bond has been integrated into photoresponsive LCs. For example, Priimagi et al. [175] paired the photoactive azo group on a halogen bond donor with an alkoxystilbazole acceptor to produce UV-active halogen bonding LCs (Figure 1.18). Separately, neither of these molecules exhibited an LC phase, but together they induced anisotropy when irradiated with polarized UV light. Replacing a C—H hydrogen bond donor in tetrafluorobenzene with an iodo halogen bond donor in iodotetrafluorobenzene resulted in a decrease of the phase-transition temperature that was dependent on the concentration of iodoperfluorobenzene, along with improved chiral light absorption [179].

The Li group doped commercially available achiral LCs with chiral halogen bonding molecular switches to produce helical cholesteric LCs (CLCs) [180]. The CLCs operate reversibly under thermal or light response. Reflection colors for these CLCs were temperature dependent, producing red, green, and blue colors. Additionally, the helical twisting power (HLC), known as the amount of chiral LC formation, could be altered by UV light interacting with the halogen bond CLCs. This concept shows that halogen bonding can be used to optimize doped LC systems to create photonic devices.

1.5.3 Supramolecular Polymers

1.5.3.1 LC Polymers

Supramolecular polymers are arrays of small molecules or linear polymeric chains held together by noncovalent interactions. LC polymers have many of

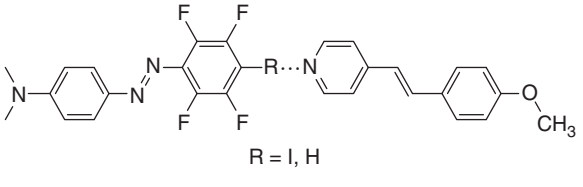

Figure 1.18 The first example of a photoactive halogen bonding LC developed by Priimagi et al.

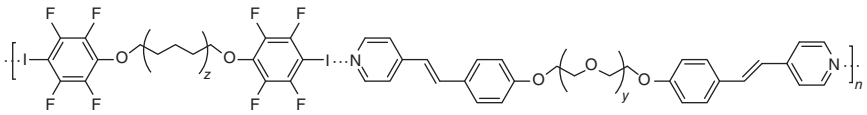

Figure 1.19 The first example of a polymeric halogen bonding LC developed by Xu. (Xu et al. [174].)

the characteristics of other polymers, including mechanical strength at high temperatures, chemical resistance, and flame resistance, while maintaining LC order. The strength and directionality of the halogen bond make it an interesting noncovalent interaction to be used in polymer science. Yet, there are very limited examples, as detailed by a review in 2012 [181]. Xu et al. created the first LC polymer mediated by halogen bonds using bis(iodotetrafluorophenoxy) alkane donors, which formed halogen bonds with nitrogen acceptors on various stilbazole derivatives (Figure 1.19) [174]. The formation temperatures of the halogen bond LCs were narrower than hydrogen bond analogues utilizing carboxyl-pyridine binding. The authors attribute the stabilization of the hydrogen bond derivatives to weak pyridine C—H hydrogen bonds to the carbonyl oxygen. A second example comes from Cho et al. who developed an alternating hydrogen bond–halogen bond [182] system, which produced a mesophase at much broader temperatures than halogen bonding analogues. The examples above highlight how the halogen bond can influences LC polymer formation; however more studies are needed to understand the role of halogen bonding in their construction.

1.5.3.2 Light-sensitive Polymers

A seminal study of light-sensitive polymers compared hydrogen and halogen bond-based azobenzene photopolymers [183]. It was found that the halogen-bonded polymers had a greater light-induced mass transport efficiency than the hydrogen bond analogues. The use of halogens did not change the photophysical or electronic properties significantly, suggesting that incorporation of halogen bond motifs into other known systems could easily modulate performance. Later studies of azobenzene polymers as light-induced surface patterning polymers show that halogen bonding species outperform hydrogen bonding ones in terms of patterning efficiency, which the authors attribute to the high directionality of the halogen bond. The efficiency was also shown to be directly proportional with halogen bond strength [184].

1.5.3.3 Block Polymers

Block copolymers consist of two or more covalently linked polymers. The Taylor lab developed a reversible addition-fragmentation chain transfer (RAFT) polymerization where amine acceptors were combined with iodoperfluorobenzene halogen bond donors, producing supramolecular diblock polymers with higher-order sphere, vesicle, and rodlike structures [176]. Similar to hydrogen bonding supramolecular diblock polymers, these formations were also highly solvent dependent. Further developments to these systems revealed that well-defined inverted vesicle morphologies could be facilitated by the hydrophobicity of the halogen bond [185].

Triblock terpolymers are another class of polymer that can form microparticles with more functional domains than diblock polymers. However, strategies to predict how triblock terpolymers assemble are in their infancy. Quintieri et al. first developed ABC 3D styrene-based triblock terpolymers utilizing the halogen bond [186]. In this study, a variety of hydroxy hydrogen bond and perfluoroiodobenzene halogen bond donors were used to form microparticles under confinement (Figure 1.20a). Interestingly, the particles formed either lamella–sphere or lamella–lamella morphologies based on the type of donor (Figure 1.20b). In general, weaker hydrogen or halogen donors lead to increased particle volume. Therefore, they found that both the donor strength and intermolecular packing interactions were important for the overall morphology of the nanoparticle.

1.5.3.4 Self-healing Polymers

Select self-healing polymers employ reversible networks of noncovalent interactions and are of topical interest for several real-world applications. For example, using halogen bonds in self-healing polymers allows for the creation of hard coatings with healing properties. The polymers are "repaired" by reorganizing noncovalent interactions to maintain structural and mechanical integrity and can sustain many healing cycles while keeping their mechanical robustness. The first examples of halogen bond self-healing polymers were developed by Schubert and Hager in 2017 [187, 188]. Cross-linking between iodotriazole and iodotriazolium halogen bond donors and tetra-*N*-butylammonium acetate polymeric salt acceptors (Figure 1.21) in these systems was revealed by a characteristic shift in the C–I band in the Raman spectrum. The self-healing behavior in these polymers was indicated by scratch-healing tests. Future studies of self-healing polymers that incorporate halogen bonding are being directed at maximizing the self-healing mechanism. Given that there are few examples, the field will likely expand to include a wider variety of self-healing polymer systems.

1.5.4 Supramolecular Gels

Low molecular weight supramolecular gels can be used for sensing, cell growth media, drug delivery, and stimuli-responsive optical/electronic materials. Hydrogen bond interactions are commonly used to form 1D or 2D fibrils that are sensitive to competing noncovalent interactions. These competing interactions can therefore be used to control gel formation or gel strength. Metrangolo and Resnati created 1,4-diiodotetrafluorobenzene and 1,4-bis(3-pyridylureido)butane mixtures whose crystal structure revealed a halogen bonding diiodoperfluorobenzene donor, pyridine acceptor, and hydrogen bonding urea donor–acceptor lattice. This combination of molecules resulted in the formation of a supramolecular polymeric gel in dimethyl sulfoxide–water mixtures [189]. This was the first example using a halogen bond to form a supramolecular gel in polar media, suggesting that halogen bonds can operate in the presence of polar solvents and be used for gel-based materials [190]. The linearity of the halogen bond has also been exploited to develop macroscale materials [191]. By using a halogen bonding 1-iodoperfluoroalkane

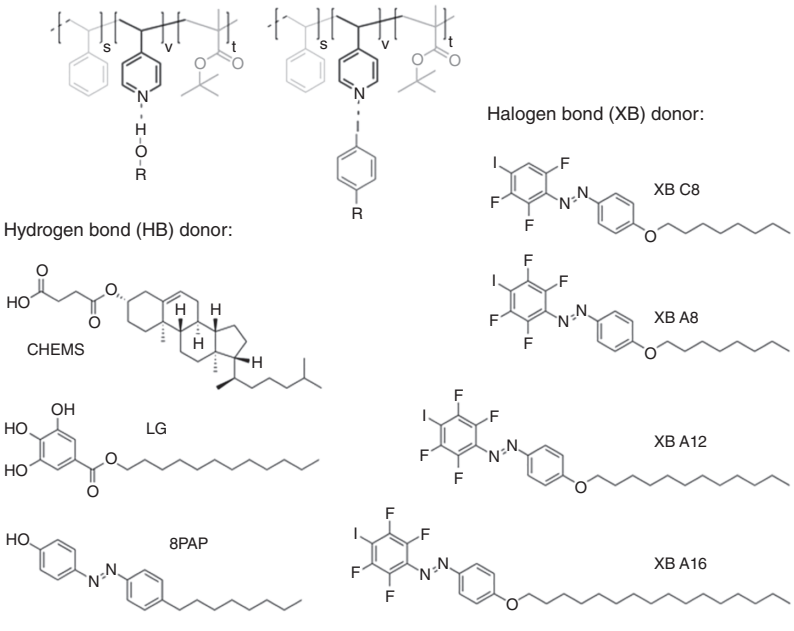

Figure 1.20 (a) Chemical structure of the halogen bond and hydrogen bond donors used in nanoparticle formation. (b) Tuning of the poly(4-vinylpyridine) (P4VP) volume with halogen bond and hydrogen bond donors and transition from lamella–sphere to lamella–lamella morphology. Source: From Quintieri et al. [186]. © 2018 MDPI.

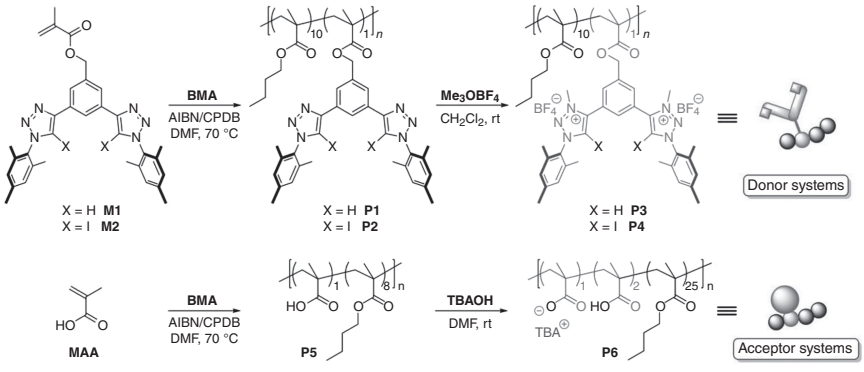

Figure 1.21 Monomers **M1** and **M2** were subjected to RAFT polymerization with butyl methacrylate (BMA) to prepare the donor-containing copolymers **P1** and **P2**, which were methylated to obtain **P3** and **P4**. Acceptor copolymers **P5** and **P6** were obtained by RAFT polymerization of BMA with methyl methacrylate (MAA) and subsequent treatment with TBAOH. Source: From Tepper et al. [187]. © 2017 John Wiley & Sons.

donor with a polyethylene glycol-based ammonium chloride end-capped acceptor, a star-shaped polymer was created, which formed millimeter-sized films without any other external templating forces. Even in the few reported systems, the halogen bond has been versatile enough to produce polymeric gels in competitive media and strong enough to generate millimeter scale assemblies.

1.5.5 Materials Conclusion

Despite the early stage of development, materials scientists have used the halogen bond to construct a diverse range of LCs, ionic liquids, self-healing polymers, and macroscopic self-assembled gels. These initial materials provide perspective for the detailed discussions of solution-based halogen bonding found in subsequent chapters. However, halogen bond-based materials are still largely inspired and derived from hydrogen bond-based materials. Surely, combining the ingenuity of the chemist with the directionality, tunability, solvent resistance, and lipophilicity of the halogen bond will produce unique materials for a variety of exciting applications. Future studies will improve the properties of halogen bonding materials and will be used to gain a greater understanding of the noncovalent interactions available to the chemist.

1.6 Conclusion

From intellectual curiosity to versatile supramolecular tool, the ascension of the halogen bond has been significant. In less than 20 years since the "rediscovery" concept article, the works of many scientists have produced a solid foundational understanding of the halogen bond. The wide breadth of fundamental studies of the halogen bond across all phases (solid, solution, gas, and *in silico*) has resulted in

extensive (and growing) application across diverse fields. Furthermore, the success of the halogen bond has inspired a renaissance of other σ-hole-type interactions (e.g. chalcogen, pnictogen, and tetrel bonds) that have developed rapidly, as concepts, nomenclature, and fundamentals parallel the halogen bond.

The rise of these noncovalent forces has expanded the supramolecular landscape. As such, readers should continue to expect comparative investigations on how the halogen bond "stacks up" against other noncovalent interactions – some of which will be discussed in later chapters. These and other fundamental studies will continue to refine our understanding of the halogen bond. As the field advances, enriched understanding and computational models will lead to improved molecular designs – the prospects of which are vast. The intent of this introduction has been to provide a deeper understanding of the halogen bond that can be used to contextualize the solution discussions found in later chapters. The following chapters highlight fundamental and functional studies of the halogen bond in solution.

Acknowledgments

O.B.B., D.A.D., and E.A.J. are thankful for the support from National Science Foundation (NSF) CAREER CHE-1555324. O.B.B., D.A.D., and E.A.J. are thankful for X-ray core facility support by the Center for Biomolecular Structure and Dynamics CoBRE (NIH NIGMS grant P20GM103546) and the University of Montana (UM).

References

1 Guo, N., Maurice, R., Teze, D. et al. (2018). *Nat. Chem.* 10: 1–7.
2 Desiraju, G.R., Ho, P.S., Kloo, L. et al. (2013). *Pure Appl. Chem.* 85: 1711–1713.
3 Von, P., Schleyer, R., and West, R. (1959). *J. Am. Chem. Soc.* 81: 3164–3165.
4 Ramasubbu, N., Parthasarathy, R., and Murray-Rust, P. (1986). *J. Am. Chem. Soc.* 108: 4308–4314.
5 Brinck, T., Murray, J.S., and Politzer, P. (1992). *Int. J. Quantum Chem.* 44: 57–64.
6 Murray, J.S., Paulsen, K., and Politzer, P. (1994). *Proc. Indian Acad. Sci.* 106: 267–275.
7 Cavallo, G., Metrangolo, P., Milani, R. et al. (2016). *Chem. Rev.* 116: 2478–2601.
8 Clark, T., Hennemann, M., Murray, J.S., and Politzer, P. (2007). *J. Mol. Model.* 13: 291–296.
9 Alvarez, S. (2013). *Dalton Trans.* 42: 8617.
10 Shannon, R.D. (1976). *Acta Crystallogr. Sect. A* 32: 751–767.
11 Metrangolo, P., Meyer, F., Pilati, T. et al. (2008). *Angew. Chem. Int. Ed.* 47: 6114–6127.
12 Priimagi, A., Cavallo, G., Metrangolo, P., and Resnati, G. (2013). *Acc. Chem. Res.* 46: 2686–2695.

13 Riel, A.M.S., Jessop, M.J., Decato, D.A. et al. (2017). *Acta Crystallogr. Sect. B Struct. Sci. Cryst. Eng. Mater.* 73: 203–209.

14 Riel, A.M.S., Rowe, R.K., Ho, E.N. et al. (2019). *Acc. Chem. Res.* 52: 2870–2880.

15 Riel, A.M.S., Decato, D.A., Sun, J. et al. (2018). *Chem. Sci.* 9: 5828–5836.

16 Carlsson, A.-C.C., Scholfield, M.R., Rowe, R.K. et al. (2018). *Biochemistry* 57: 4135–4147.

17 Bent, H.A. (1968). *Chem. Rev.* 68: 587–648.

18 Lu, Y.X., Zou, J.W., Yu, Q.S. et al. (2007). *Chem. Phys. Lett.* 449: 6–10.

19 Laurence, C., Graton, J., and Gal, J.F. (2011). *J. Chem. Educ.* 88: 1651–1657.

20 Karan, N.K. and Arunan, E. (2004). *J. Mol. Struct.* 688: 203–205.

21 Raghavendra, B. and Arunan, E. (2007). *J. Phys. Chem. A* 111: 9699–9706.

22 Urinda, S., Kundu, D., and Majee, A. (2009). *Heteroat. Chem.* 20: 232–234.

23 Imakubo, T., Tajima, N., Shirahata, T. et al. (2003). *Synth. Met.* 135–136: 601–602.

24 Laurence, C., Graton, J., Berthelot, M., and El Ghomari, M.J. (2011). *Chem. Eur. J.* 17: 10431–10444.

25 Lieffrig, J., Jeannin, O., Frąckowiak, A. et al. (2013). *Chem. -Eur. J.* 19: 14804–14813.

26 Cametti, M., Raatikainen, K., Metrangolo, P. et al. (2012). *Org. Biomol. Chem.* 10: 1329–1333.

27 Gilday, L.C., Lang, T., Caballero, A. et al. (2013). *Angew. Chem. Int. Ed.* 52: 4356–4360.

28 Zapata, F., Caballero, A., White, N.G. et al. (2012). *J. Am. Chem. Soc.* 134: 11533–11541.

29 Walter, S.M., Kniep, F., Rout, L. et al. (2012). *J. Am. Chem. Soc.* 134: 8507–8512.

30 Kassl, C.J., Swenson, D.C., and Pigge, F.C. (2015). *Cryst. Growth Des.* 15: 4571–4580.

31 Sabater, P., Zapata, F., Caballero, A. et al. (2016). *J. Org. Chem.* 81: 7448–7458.

32 Carlsson, A.-C.C., Gräfenstein, J., Budnjo, A. et al. (2012). *J. Am. Chem. Soc.* 134: 5706–5715.

33 Carlsson, A.-C.C., Gräfenstein, J., Laurila, J.L. et al. (2012). *Chem. Commun.* 48: 1458–1460.

34 Carlsson, A.-C.C., Uhrbom, M., Karim, A. et al. (2013). *CrystEngComm* 15: 3087.

35 Rosenfeld, L. (2000). *J. Chem. Educ.* 77: 984.

36 Colin, M. (1814). *Ann. Chim.* 91: 252–272.

37 Guthrie, F. (1863). *J. Chem. Soc.* 16: 239–244.

38 Remsen, I. and Norris, J.F. (1896). *Am. Chem. J.* 18: 90–95.

39 Rhoussopoulos, O. (1883). *Ber. Dtsch. Chem. Ges.* 16: 202–203.

40 Lachman, A. (1903). *J. Am. Chem. Soc.* 25: 50–55.

41 Benesi, H.A. and Hildebrand, J.H. (1948). *J. Am. Chem. Soc.* 70: 2832–2833.

42 Mulliken, R.S. (1950). *J. Am. Chem. Soc.* 72: 600–608.

43 Mulliken, R.S. (1966) Spectroscopy, molecular orbitals, and chemical bonding. Nobel Lecture.

44 Hassel, O., Hvoslef, J., Vihovde, E.H., and Sörensen, N.A. (1954). *Acta Chem. Scand.* 8: 873–873.

45 Hassel, O., Strømme, K.O., Haraldsen, H. et al. (1958). *Acta Chem. Scand.* 12: 1146–1146.

46 Hassel, O., Strømme, K.O., Hammarsten, E. et al. (1959). *Acta Chem. Scand.* 13: 1781–1786.

47 Hassel, O., Strømme, K.O., Stenhagen, E. et al. (1959). *Acta Chem. Scand.* 13: 275–280.

48 Hassel, O. (1970) Structural aspects of interatomic charge-transfer bonding. Nobel Lecture.

49 Dumas, J.M., Gomel, M., and Guerin, M. (2010). *Patai Suppl. D, Chem. Halides Pseudo-Halides Azides* 2: 985–1020.

50 Schulz, N., Sokkar, P., Engelage, E. et al. (2018). *Chem. Eur. J.* 24: 3464–3473.

51 Legon, A.C. (1998). *Chem. Eur. J.*: 4, 1890–1897.

52 Legon, A.C. (1999). *Angew. Chem. Int. Ed.* 38: 2686–2714.

53 Weiss, R., Rechinger, M., Hampel, F., and Wolski, A. (1995). *Angew. Chem. Int. Ed.* 34: 441–443.

54 Weiss, R., Miess, G.-E., Haller, A., and Reinhardt, W. (1986). *Angew. Chem. Int. Ed.* 25: 103–104.

55 Weiss, R., Rechinger, M., and Hampel, F. (1994). *Angew. Chem. Int. Ed.* 33: 893–895.

56 Metrangolo, P., Neukirch, H., Pilati, T., and Resnati, G. (2005). *Acc. Chem. Res.* 38: 386–395.

57 Metrangolo, P. and Resnati, G. (2001). *Chem. Eur. J.* 7: 2511–2519.

58 Li, B., Zang, S.Q., Wang, L.Y., and Mak, T.C.W. (2016). *Coord. Chem. Rev.* 308: 1–21.

59 Fourmigué, M. (2009). *Curr. Opin. Solid State Mater. Sci.* 13: 36–45.

60 Ding, X., Tuikka, M., and Haukk, M. (2012). *Recent Advances in Crystallography*, vol. i, 13. InTech.

61 Christopherson, J.C., Topić, F., Barrett, C.J., and Friščić, T. (2018). *Cryst. Growth Des.* 18: 1245–1259.

62 Mukherjee, A., Tothadi, S., and Desiraju, G.R. (2014). *Acc. Chem. Res.* 47: 2514–2524.

63 Gilday, L.C., Robinson, S.W., Barendt, T.A. et al. (2015). *Chem. Rev.* 115: 7118–7195.

64 Aakeröy, C.B. and Spartz, C.L. (2015). *Halogen Bonding I: Impact on Materials Chemistry and Life Sciences* (eds. P. Metrangolo and G. Resnati), 155–182. Cham: Springer International Publishing.

65 Metrangolo, P., Resnati, G., Pilati, T., and Biella, S. (2008). *Halogen Bonding: Fundamentals and Applications* (eds. P. Metrangolo and G. Resnati), 105–136. Berlin, Heidelberg: Springer Berlin Heidelberg.

66 Murray-Rust, P. and Motherwell, W.D.S. (1979). *J. Am. Chem. Soc.* 101: 4374–4376.

67 Lommerse, J.P.M., Stone, A.J., Taylor, R., and Allen, F.H. (1996). *J. Am. Chem. Soc.* 118: 3108–3116.

68 Desiraju, G.R. and Parthasarathy, R. (1989). *J. Am. Chem. Soc.* 111: 8725–8726.

69 Pedireddi, V.R., Reddy, D.S., Goud, B.S. et al. (1994). *J. Chem. Soc., Perkin Trans.* 2: 2353.

70 Chopra, D. (2012). *Cryst. Growth Des.* 12: 541–546.

71 Präsang, C., Whitwood, A.C., and Bruce, D.W. (2009). *Cryst. Growth Des.* 9: 5319–5326.

72 Aakeröy, C.B., Baldrighi, M., Desper, J. et al. (2013). *Chem. Eur. J.* 19: 16240–16247.

73 Etter, M.C. (1990). *Acc. Chem. Res.* 23: 120–126.

74 Aakery, C.B., Beatty, A.M., and Helfrich, B.A. (2001). *Angew. Chem. Int. Ed.* 40: 3240–3242.

75 Aakeröy, C.B., Wijethunga, T.K., Desper, J., and Daković, M. (2016). *Cryst. Growth Des.* 16: 2662–2670.

76 Aakeröy, C.B., Spartz, C.L., Dembowski, S. et al. (2015). *IUCrJ* 2: 498–510.

77 Aakeröy, C.B., Chopade, P.D., and Desper, J. (2011). *Cryst. Growth Des.* 11: 5333–5336.

78 Aakeröy, C.B., Chopade, P.D., Ganser, C., and Desper, J. (2011). *Chem. Commun.* 47: 4688–4690.

79 Tothadi, S. and Desiraju, G.R. (2013). *Chem. Commun.* 49: 7791–7793.

80 Voth, A.R., Khuu, P., Oishi, K., and Ho, P.S. (2009). *Nat. Chem.* 1: 74–79.

81 Vasylyeva, V., Nayak, S.K., Terraneo, G. et al. (2014). *CrystEngComm* 16: 8102–8105.

82 Takemura, A., McAllister, L.J., Hart, S. et al. (2014). *Chem. Eur. J.* 20: 6721–6732.

83 Decato, D.A. and Berryman, O.B. (2018). Simultaneous halogen and hydrogen bonding to carbonyl and thiocarbonyl functionality. In: *Multi-Component Crystals*, vol. 1 (eds. E. Tiekink and J. Zukerman), 272–288. Berlin, Boston: De Gruyter.

84 Logothetis, T.A., Meyer, F., Metrangolo, P. et al. (2004). *New J. Chem.* 28: 760–763.

85 Lisac, K. and Cinčić, D. (2018). *CrystEngComm* 20: 5955–5963.

86 Puttreddy, R., Peuronen, A., Lahtinen, M., and Rissanen, K. (2019). *Cryst. Growth Des.* 19: 3815–3824.

87 Ding, X., Tuikka, M., Rissanen, K., and Haukka, M. (2019). *Crystals* 9: 319.

88 Puttreddy, R., von Essen, C., and Rissanen, K. (2018). *Eur. J. Inorg. Chem.* 2018: 2393–2398.

89 Smart, P., Bejarano-Villafuerte, Á., and Brammer, L. (2013). *CrystEngComm* 15: 3151.

90 Brammer, L., Mínguez Espallargas, G., and Adams, H. (2003). *CrystEngComm* 5: 343–345.

91 Mínguez Espallargas, G., Zordan, F., Arroyo Marín, L. et al. (2009). *Chem. Eur. J.* 15: 7554–7568.

92 Zordan, F., Brammer, L., and Sherwood, P. (2005). *J. Am. Chem. Soc.* 127: 5979–5989.

93 Libri, S., Jasim, N.A., Perutz, R.N., and Brammer, L. (2008). *J. Am. Chem. Soc.* 130: 7842–7844.

94 Smith, D.A., Brammer, L., Hunter, C.A., and Perutz, R.N. (2014). *J. Am. Chem. Soc.* 136: 1288–1291.

95 Ormond-Prout, J.E., Smart, P., and Brammer, L. (2012). *Cryst. Growth Des.* 12: 205–216.

96 Carter, K.P., Kalaj, M., Surbella, R.G. et al. (2017). *Chem. Eur. J.* 23: 15355–15369.

97 Carter, K.P., Kalaj, M., Kerridge, A., and Cahill, C.L. (2018). *CrystEngComm* 20: 4916–4925.

98 Lieffrig, J., Jeannin, O., Guizouarn, T. et al. (2012). *Cryst. Growth Des.* 12: 4248–4257.

99 Lieffrig, J., Jeannin, O., Shin, K.-S. et al. (2012). *Crystals* 2: 327–337.

100 Espallargas, G.M., Recuenco, A., Romero, F.M. et al. (2012). *CrystEngComm* 14: 6381.

101 Pang, X., Zhao, X.R., Wang, H. et al. (2013). *Cryst. Growth Des.* 13: 3739–3745.

102 Boubekeur, K., Syssa-Magalé, J.-L., Palvadeau, P., and Schöllhorn, B. (2006). *Tetrahedron Lett.* 47: 1249–1252.

103 Clemente-Juan, J.M., Coronado, E., Mínguez Espallargas, G. et al. (2010). *CrystEngComm* 12: 2339.

104 Troff, R.W., Mäkelä, T., Topić, F. et al. (2013). *Eur. J. Org. Chem.* 2013: 1617–1637.

105 Makhotkina, O., Lieffrig, J., Jeannin, O. et al. (2015). *Cryst. Growth Des.* 15: 3464–3473.

106 Raatikainen, K. and Rissanen, K. (2011). *CrystEngComm* 13: 6972.

107 Mavračić, J., Cinčić, D., and Kaitner, B. (2016). *CrystEngComm* 18: 3343–3346.

108 Stilinović, V., Horvat, G., Hrenar, T. et al. (2017). *Chem. Eur. J.* 23: 5244–5257.

109 Eraković, M., Cinčić, D., Molčanov, K., and Stilinović, V. (2019). *Angew. Chem. Int. Ed.* 58: 15702–15706.

110 Caronna, T., Liantonio, R., Logothetis, T.A. et al. (2004). *J. Am. Chem. Soc.* 126: 4500–4501.

111 Sinnwell, M.A., Blad, J.N., Thomas, L.R., and MacGillivray, L.R. (2018). *IUCrJ* 5: 491–496.

112 Sinnwell, M.A. and MacGillivray, L.R. (2016). *Angew. Chem. Int. Ed.* 55: 3477–3480.

113 DeCicco, R.C., Luo, L., and Goroff, N.S. (2019). *Acc. Chem. Res.* 52: 2080–2089.

114 Cinčić, D., Friščić, T., and Jones, W. (2008). *J. Am. Chem. Soc.* 130: 7524–7525.

115 Cavallo, G., Metrangolo, P., Pilati, T. et al. (2010). *Chem. Soc. Rev.* 39: 3772–3783.

116 Metrangolo, P., Pilati, T., Terraneo, G. et al. (2009). *CrystEngComm* 11: 1187–1196.

117 Xu, Y., Gabidullin, B., and Bryce, D.L. (2019). *J. Phys. Chem. A* 123: 6194–6209.

118 Szell, P.M.J., Grébert, L., and Bryce, D.L. (2019). *Angew. Chem. Int. Ed.* 58: 13479–13485.

119 Shankar, S., Chovnik, O., Shimon, L.J.W. et al. (2018). *Cryst. Growth Des.* 18: 1967–1977.

120 Syssa-Magalé, J.-L., Boubekeur, K., Leroy, J. et al. (2014). *CrystEngComm* 16: 10380–10384.

121 Titi, H.M., Nandi, G., Tripuramallu, B.K., and Goldberg, I. (2015). *Cryst. Growth Des.* 15: 3063–3075.

122 Catalano, L., Perez-Estrada, S., Wang, H.-H. et al. (2017). *J. Am. Chem. Soc.* 139: 843–848.

123 Simonov, S., Zorina, L., Wzietek, P. et al. (2018). *Nano Lett.* 18: 3780–3784.

124 Müller, M., Albrecht, M., Gossen, V. et al. (2010). *Chem. Eur. J.* 16: 12446–12453.

125 García, M.D., Martí-Rujas, J., Metrangolo, P. et al. (2011). *CrystEngComm* 13: 4411.

126 Peuronen, A., Rinta, H., and Lahtinen, M. (2015). *CrystEngComm* 17: 1736–1740.

127 Szell, P.M.J., Gabriel, S.A., Caron-Poulin, E. et al. (2018). *Cryst. Growth Des.* 18: 6227–6238.

128 Widner, D.L., Knauf, Q.R., Merucci, M.T. et al. (2014). *J. Org. Chem.* 79: 6269–6278.

129 Politzer, P., Lane, P., Concha, M.C. et al. (2007). *J. Mol. Model.* 13: 305–311.

130 Politzer, P., Murray, J.S., and Clark, T. (2013). *Phys. Chem. Chem. Phys.* 15: 11178.

131 Frontera, A., Gamez, P., Mascal, M. et al. (2011). *Angew. Chem. Int. Ed.* 50: 9564–9583.

132 Wolters, L.P., Schyman, P., Pavan, M.J. et al. (2014). *Wiley Interdiscip. Rev. Comput. Mol. Sci.* 4: 523–540.

133 Kolář, M.H. and Hobza, P. (2016). *Chem. Rev.* 116: 5155–5187.

134 Sedlak, R., Kolář, M.H., and Hobza, P. (2015). *J. Chem. Theor. Comput.* 11: 4727–4732.

135 Nyburg, S.C. and Faerman, C.H. (1985). *Acta Crystallogr. Sect. B Struct. Sci.* 41: 274–279.

136 Hathwar, V.R. and Guru Row, T.N. (2011). *Cryst. Growth Des.* 11: 1338–1346.

137 Chopra, D. (2012). *J. Phys. Chem. A* 116: 9791–9801.

138 Murray, J.S. and Politzer, P. (2011). *Wiley Interdiscip. Rev. Comput. Mol. Sci.* 1: 153–163.

139 Riley, K.E., Murray, J.S., Fanfrlík, J. et al. (2011). *J. Mol. Model.* 17: 3309–3318.

140 Politzer, P. and Murray, J.S. (2017). *Crystals* 7: 212.

141 Brinck, T., Murray, J.S., and Politzer, P. (1993). *Int. J. Quantum Chem.* 48: 73–88.

142 Murray, J.S., Macaveiu, L., and Politzer, P. (2014). *J. Comput. Sci.* 5: 590–596.

143 Riley, K.E., Murray, J.S., Politzer, P. et al. (2009). *J. Chem. Theor. Comput.* 5: 155–163.

144 Aakeröy, C.B., Wijethunga, T.K., and Desper, J. (2014). *J. Mol. Struct.* 1072: 20–27.

145 Sarwar, M.G., Dragisic, B., Salsberg, L.J. et al. (2010). *J. Am. Chem. Soc.* 132: 1646–1653.
146 Beale, T.M., Chudzinski, M.G., Sarwar, M.G., and Taylor, M.S. (2013). *Chem. Soc. Rev.* 42: 1667–1680.
147 Huber, S.M., Jimenez-Izal, E., Ugalde, J.M., and Infante, I. (2012). *Chem. Commun.* 48: 7708.
148 Palusiak, M. (2010). *J. Mol. Struct.-THEOCHEM* 945: 89–92.
149 Wolters, L.P. and Bickelhaupt, F.M. (2012). *ChemistryOpen* 1: 96–105.
150 Alkorta, I., Rozas, I., and Elguero, J. (1998). *J. Phys. Chem. A* 102: 9278–9285.
151 Rosokha, S.V., Stern, C.L., and Ritzert, J.T. (2013). *Chem. Eur. J.* 19: 8774–8788.
152 Rosokha, S.V., Stern, C.L., Swartz, A., and Stewart, R. (2014). *Phys. Chem. Chem. Phys.* 16: 12968–12979.
153 Riley, K.E. and Hobza, P. (2013). *Phys. Chem. Chem. Phys.* 15: 17742.
154 Eskandari, K. and Zariny, H. (2010). *Chem. Phys. Lett.* 492: 9–13.
155 Riley, K.E. and Hobza, P. (2008). *J. Chem. Theor. Comput.* 4: 232–242.
156 Jeziorski, B., Moszynski, R., and Szalewicz, K. (1994). *Chem. Rev.* 94: 1887–1930.
157 Williams, H.L. and Chabalowski, C.F. (2001). *J. Phys. Chem. A* 105: 646–659.
158 Valadares, N.F., Salum, L.B., Polikarpov, I. et al. (2009). *J. Chem. Inf. Model.* 49: 2606–2616.
159 Auffinger, P., Hays, F.A., Westhof, E., and Ho, P.S. (2004). *Proc. Natl. Acad. Sci. USA* 101: 16789–16794.
160 Xu, Z., Yang, Z., Liu, Y. et al. (2014). *J. Chem. Inf. Model.* 54: 69–78.
161 Ford, M.C. and Ho, P.S. (2016). *J. Med. Chem.* 59: 1655–1670.
162 Rezac, J. and Hobza, P. (2011). *Chem. Phys. Lett.* 506: 286–289.
163 Dobeš, P., Řezáč, J., Fanfrlík, J. et al. (2011). *J. Phys. Chem. B* 115: 8581–8589.
164 Zimmermann, M.O., Lange, A., and Boeckler, F.M. (2015). *J. Chem. Inf. Model.* 55: 687–699.
165 Lu, Y., Shi, T., Wang, Y. et al. (2009). *J. Med. Chem.* 52: 2854–2862.
166 Jorgensen, W.L. and Schyman, P. (2012). *J. Chem. Theor. Comput.* 8: 3895–3901.
167 Case, D.A., Cheatham, T.E., Darden, T. et al. (2005). *J. Comput. Chem.* 26: 1668–1688.
168 Carter, M., Rappé, A.K., and Ho, P.S. (2012). *J. Chem. Theor. Comput.* 8: 2461–2473.
169 Saccone, M. and Catalano, L. (2019). *J. Phys. Chem. B* 123: 9281–9290.
170 Paleos, C.M. and Tsiourvas, D. (2001). *Liq. Cryst.* 28: 1127–1161.
171 Wang, H., Bisoyi, H.K., Urbas, A.M. et al. (2019). *Chem. Eur. J.* 25: 1369–1378.
172 Nguyen, H.L., Horton, P.N., Hursthouse, M.B. et al. (2004). *J. Am. Chem. Soc.* 126: 16–17.
173 Cavallo, G., Terraneo, G., Monfredini, A. et al. (2016). *Angew. Chem. Int. Ed.* 55: 6300–6304.
174 Xu, J., Liu, X., Lin, T. et al. (2005). *Macromolecules* 38: 3554–3557.
175 Priimagi, A., Saccone, M., Cavallo, G. et al. (2012). *Adv. Mater.* 24: OP345–OP352.
176 Vanderkooy, A. and Taylor, M.S. (2015). *J. Am. Chem. Soc.* 137: 5080–5086.

177 McAllister, L.J., Präsang, C., Wong, J.P.W. et al. (2013). *Chem. Commun.* 49: 3946.
178 Saccone, M., Palacio, F.F., Cavallo, G. et al. (2017). *Faraday Discuss.* 203: 407–422.
179 Vapaavuori, J., Siiskonen, A., Dichiarante, V. et al. (2017). *RSC Adv.* 7: 40237–40242.
180 Wang, H., Bisoyi, H.K., Wang, L. et al. (2018). *Angew. Chem. Int. Ed.* 57: 1627–1631.
181 Berger, G., Soubhye, J., and Meyer, F. (2012). *Polym. Chem.* 19: 3559–3580.
182 Cho, C.M., Wang, X., Li, J.J. et al. (2013). *Liq. Cryst.* 40: 185–196.
183 Priimagi, A., Cavallo, G., Forni, A. et al. (2012). *Adv. Funct. Mater.* 22: 2572–2579.
184 Saccone, M., Dichiarante, V., Forni, A. et al. (2015). *J. Mater. Chem. C* 3: 759–768.
185 Vanderkooy, A. and Taylor, M.S. (2017). *Faraday Discuss.* 203: 285–299.
186 Quintieri, G., Saccone, M., Spengler, M. et al. (2018). *Nanomaterials* 8: 1029.
187 Tepper, R., Bode, S., Geitner, R. et al. (2017). *Angew. Chem. Int. Ed.* 56: 4047–4051.
188 Dahlke, J., Tepper, R., Geitner, R. et al. (2018). *Polym. Chem.* 9: 2193–2197.
189 Meazza, L., Foster, J.A., Fucke, K. et al. (2013). *Nat. Chem.* 5: 42–47.
190 Robertson, C.C., Perutz, R.N., Brammer, L., and Hunter, C.A. (2014). *Chem. Sci.* 5: 4179–4183.
191 Houbenov, N., Milani, R., Poutanen, M. et al. (2014). *Nat. Commun.* 5: 4043.